(54) Title: AN INSPECTION SYSTEM FOR A CONDUIT
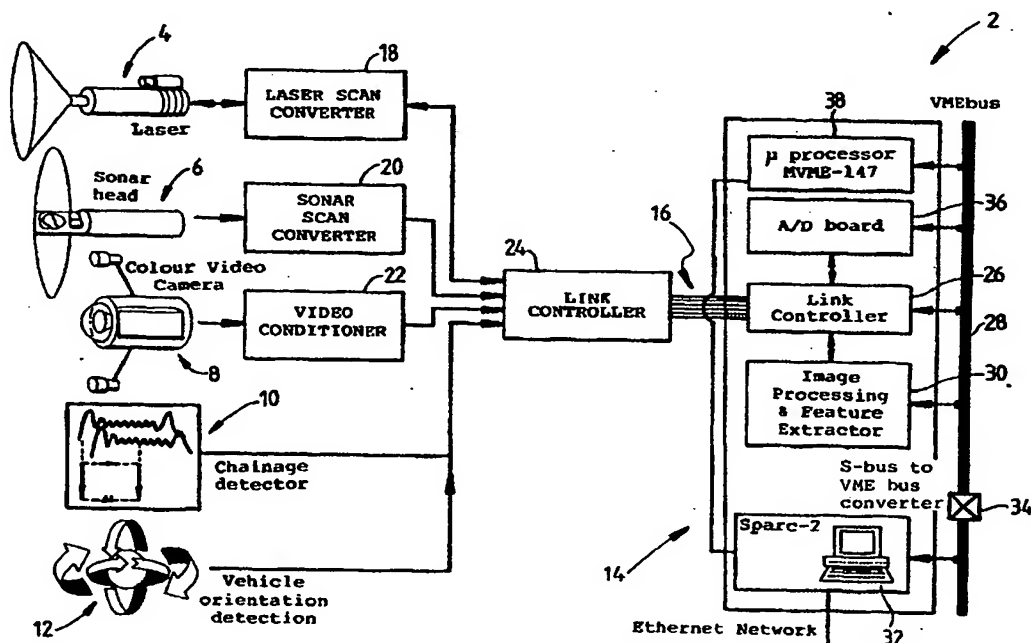
(57) Abstract

An inspection system for a conduit comprising measurement means for travelling in the conduit and obtaining data on the conduit, and processing means for processing the data to identify regions of the conduit corresponding to defects in the conduit. The measurement means may be laser scanning means and sonar scanning means.

AN INSPECTION SYSTEM FOR A CONDUIT

The present invention relates to an inspection system for a conduit. The system
5   is particularly advantageous for use in inspecting pipes, such as sanitary and storm water
sewers, but can also be adapted for inspection of other conduits, for example tunnels and
drains, in particular those used in water supply, sewerage, irrigation and drainage systems.

The inspection and assessment of sewers for defects is critical to maintain an
10   effective sewerage system. The task is of a particular importance for the world's larger
and older cities where demand on the system is high and the main sewers used have aged
considerably, thereby providing conditions conducive to the production of potentially
serious defects.

15   Sewers are presently inspected using a closed circuit television camera which is
mounted on a trolley configured to travel within the length of a pipe. The images
obtained by the camera are assessed by experienced personnel who identify defects and
potential defects in the pipe's structure on the basis of the images. Personnel can also be
sent into pipes which are large enough for direct inspection, however, this is normally
20   discouraged as, although safety precautions are stringent, there remains inherent risks t
personnel. Both assessment techniques are highly subjective and open to different
interpretations. Reliance on visual assessment is also time consuming and places
considerable time constraints on an inspection program when the number of experienced
personnel available is limited.
25

Both techniques also require inspections to be undertaken at low flow levels or
fluid flow to be diverted from the pipes being inspected. This places constraints on the
effectiveness of the sewage system and normally means that inspection programs have
to be carried out at night, thereby increasing the labour cost of the program.
30

Sonar systems have been used to inspect flooded pipes, but the images produced
from sonar systems still need to be manually interpreted.

- 2 -

In accordance with the present invention there is provided an inspection system for a conduit comprising measurement means for travelling in said conduit and obtaining data on said conduit, and processing means for processing said data to identify regions of said conduit corresponding to defects in said conduit.

5

Preferably said processing means includes means for extracting dimension data on said conduit from said data obtained by said measurement means.

Preferably said processing means includes segmentation means for processing said dimension data into segments which represent regions which could correspond to defects in said conduit. The processing means also preferably includes classification means for processing said segments to classify said segments as corresponding to a feature of said conduit, which may be a defect.

10

15

Preferably said classification means implements a neural network to classify said segments. Advantageously the system further includes interpretation means for processing a classified segment to obtain attributes of the corresponding feature and for identifying said feature on the basis of said attributes and feature data.

20

Preferably said dimension data comprises a plurality of circumferential data of the inner surface of said conduit each corresponding to points along the path of travel of said measurement means.

The measurement means may include laser scanning means and/or sonar scanning means.

25

Preferably the laser scanning means includes a laser, means for circulating a beam generated by the laser against the surface of said conduit, and camera means for producing image data representative of areas illuminated by said beam.

30

Preferably said sonar scanning means includes a rotating sonar transducer for emitting sonar signals to and receiving sonar echoes from the inner surface of said

- 3 -

conduit.

Preferably said processing means includes movement correction means for adjusting said circumferential data to account for movement of said measurement means
5   within said conduit.

A preferred embodiment of the present invention is hereinafter described, by way of example only, with reference to the accompanying drawings, wherein:

Figure 1 is a schematic diagram of an inspection system for a pipe;

10   Figure 2 is a perspective view of a laser scanner of the system within a pipe;

Figure 3 is a block diagram of a feature extraction board of the system;

Figure 4 is a block diagram of an MIS of the system;

Figure 5 is a perspective view of a sonar scanner of the system within a pipe;

Figure 6 is a block diagram of a sonar head of the sonar scanner;

15   Figure 7 is a graphical representation of a sonar echo produced by the sonar head;

Figure 8 is a frequency response of a digital filter used in processing the sonar echoes received by the sonar head;

Figure 9 is a graphical representation of a curve-fitted to a set of sonar echo samples;

20   Figure 10 is a graphical representation of a standard sonar echo used in cross-correlation of measured sonar echoes;

Figure 11 is a graphical representation of the results achieved by cross-correlation of the standard sonar echo with a measured sonar echo;

Figure 12 is a flow diagram of image processing software modules and databases
25   of a work station of the system;

Figure 13 is a flow diagram of an image segmentation module of the system;

Figure 14 is a flow diagram of an image classification module of the system;

Figure 15 is a diagram of a grid representing a triangulation step of the image classification module;

30   Figure 16 is a diagram of a neural network structure used in the image classification module;

Figure 17 is a flow diagram of an image interpretation module of the system;

– 4 –

Figur 18 is a diagram illustrating the coordinate axis of a vehicle in a pipe;

Figure 19 is a diagram of coordinates for a general ellipse.

Figure 20 is a diagram illustrating determination of vehicle yaw and pitch angles from a fitted ellipse; and

5   Figure 21 is a diagram illustrating centre coordinate correction.

A pipe inspection system 2, as shown in Figure 1, includes a laser scanner 4, a sonar scanner 6, and a colour video camera 8 which are all mounted on a measurement vehicle 40 that can travel within a pipe, such as a sewage pipe. The measurement vehicle

10   is self–propelled for movement through the pipe, and a chainage detector 10 is used to detect incremental movement of the measurement vehicle through the pipe, which enables the position of the measurement vehicle along the length of the pipe to be determined. The orientation of the measurement vehicle, and the scanning equipment 4 to 8, is determined by an orientation detector 12 which is also mounted on the measurement

15   vehicle. The orientation detector 12 includes a gyroscope and accelerometers. The signals generated by the measurement and detection equipment 4 to 12 of the vehicle are sent to a processing system 14 of the inspection system 2 via a high speed communications link 16. The signals from the laser scanner 4, sonar scanner 6 and colour video camera 8 are placed in a form suitable for transmission by a laser scan

20   converter 18, a sonar scan converter 20 and a video conditioner 22, respectively. Signals from the chainage detector 10, the orientation detector 12 and auxiliary sensors are combined and placed in a form suitable for transmission by a sensor conditioner 23. All the signals are combined by a link controller 24 mounted on the vehicle and which is connected to the link 16. The link 16 is an optical fibre link, and the converters 18 and

25   20 and the conditioners 22 and 23 digitise the signals produced by the scanners 4 and 6 and the camera 8 prior to submission to the link controller 24. The link controller 24 is then used to time division multiplex the digital signals and convert them to optical signals for transmission on the link 16.

30   The processing system 14 can be placed outside the pipe and connected directly to the link 16 or alternatively the signals on the link 16 can be transferred over a digital telecommunications network to a remote location of the processing system 14. The

- 5 -

processing system 14 includes a link controller 26 connected to the link 16 which is used to unpack or demultiplex the signals transmitted from the measurement vehicle. The link controller 26 is connected to other components of the processing system 14 by a VME (Versa Module Europe) bus architecture 28. The signals from the scanner 4 are passed

5   to image processing and feature extraction circuitry 30 which records the signals obtained for each inner circumferential scan of the pipe at each longitudinal position, z, of the measurement vehicle. The signals are processed to obtain circumferential or ring data for each position z, which comprises a set of x,y or r,θ coordinates defining the inner circumferential dimensions of the pipe. A Sun Microsystems Sparc-2 work station 32

10   is connected to the VME bus 28 by a VME bus to S bus converter 34, and is used to process the ring data to form feature segments and then classify the segments to determine if they correspond to a defect in the pipe structure. The processing system 14 further includes an A/D board 36 for digitising the signals from other analog sensors external to the pipe, and a Motorola MV 147 central processing unit 38 which is used to

15   control the data flow in processing system 14 and operate the scanners and detectors 4 to 12 in real-time. Ring data for each position z is also derived from the signals provided by sonar scanner 6.

The laser scanner 4 is used to obtain ring data 4 for empty pipes or the upper

20   non-fluid sections of part full pipes. The sonar scanner 6 is complementary, and is used to obtain ring data for full pipes or the lower fluid sections of partly full pipes. The colour video camera 8 is used to obtain visual images of the inside of the pipe which are recorded onto video tape and can be used for subsequent visual inspection of sections of the pipe, if desired.

25

The laser scanner 4, as shown in Figure 2 mounted on the measurement vehicle 40 within a pipe 42, includes a HeNe laser 44 which generates a laser beam 46 in the direction of travel of the support vehicle 40 substantially parallel to the axis of the pipe 42. The beam 46 is emitted from a first end 48 of the laser 44 to which a mirror 50 is

30   attached which directs the beam 46 onto a refracting prism 52. The prism 52 directs the beam 46 in a radial direction onto the inner surface of the pipe 42. The prism 52 is rotated by a stepper motor 54, mounted on top of the laser 44, so as to sweep the beam

- 6 -

46 in a circular path across inner circumferences of the pipe 42. The prism 52 completes a revolution every 20 milliseconds, and a complete trace 55 of the beam 46 is imaged at each position z of a support vehicle 40 by a CCD camera 56 mounted on the laser 44 at the back end 58 of the laser 44. The position z of the support vehicle 44 for each trace

5   55 is measured by the chainage detector 10, which comprises an optical encoder m unted on a sprocket which transfers the drive of an electric motor to the measurement vehicle 40 as it moves longitudinally along the pipe 42. The trace 55 provides an accurate representation of the form of the inner surface of the pipe 42, at a position z from which x,y or r,θ coordinates representative of the surface dimensions can be extracted, bearing

10   in mind the trace 55 is substantially perpendicular to the pipe axis.

     The image processing and feature extraction circuit 30 includes a feature extractor board 62 which receives the image signals generated by the CCD camera 56 of the laser scanner 4, as shown in Figure 3. The board 62 includes a timing generation circuit 64

15   which provides vertical and horizontal synchronising (sync) signals to the camera 56. The sync signals are generated by a video sync generator 66 based on a 28.375 MHz clock signal generated by a two phase clock generator 68. The clock generator 68 generates two 28.375 MHz clock signals which are 90° out of phase, the first being inputted to the video sync generator 66. The clock generator 68 generates the clock

20   signals from a 56.75 MHz master clock 70.

     The feature extraction board 62 further includes a video processing circuit 72, a feature store control and an addressing circuit 74, a feature data generation circuit 76, a feature storage circuit 78, and an interface 80 to the VME bus 28. The video processing

25   circuit 72 includes a camera interface 82 which buffers the video signal output by the CCD camera 56. The level of the video signal is compared by an analog comparator 86 with the level of a threshold signal generated by a threshold generator 84 to determine whether the video signal corresponds to a pixel of the imaged laser beam trace 55. The comparator 86 will produce a high signal if the video signal exceeds the threshold

30   indicating that the incident signal corresponds to a pixel of the trace 55, otherwise a low signal is produced at the output of the comparator 86. The timing of the output of the comparator 86 is controlled by the first clock signal.

The feature store control addressing circuit 74 includes feature store control logic 88 and an address counter 90. The feature store control logic 88 receives the output of the comparator 86 and its timing is controlled by the first and second clock signals generated by the timing generation circuit 64. The feature store control logic 88 enables

5   a write operation to the feature storage circuit 78 when the output of the comparator 86 provides a high signal. The write operation occurs at the address provided by the address counter 90 and the data written to that location is the contents of a pixel counter 92 and a line counter 94 of the feature data generation circuit 76. The line counter 94 provides the number of the horizontal line of the current pixel corresponding to the video signal

10   output by the camera interface 82, and the pixel counter 92 provides the number of the current pixel in that line. The pixel counter 92 is incremented by the second clock signal, and reset by the horizontal sync signal whereas the line counter 94 is incremented by the horizontal sync signal and reset by the vertical sync signal. The pixel counter 92 and the line counter 94 therefore provide x and y position data, respectively, for the current pix 1,

15   which is only stored in the storage circuit 78 when the current pixel corresponds to a pixel of the laser trace 55. The feature store control logic 88 increments the address in the address counter 90 after performing each write operation. The contents f the counters 92 and 94 form a 32-bit word which is stored in the storage circuit 78.

20   The feature storage circuit 78 is a dual port RAM which can hold 32 K 32-bit words and is split into two banks for double buffer operation, i.e. one bank is written to while the other bank is read by the VME interface 80. The feature store control logic 88 controls the double buffer operation by ensuring that when one bank is full, a read signal is provided to the VME interface 80, and then the write operation continues at the other

25   bank. An error signal to the VME interface 80 is generated when the read operation to one bank is not finished yet the other bank is full of x,y data. The VME interface 80 controls the reading of data onto the VME bus, and the feature extraction board 62 function as a slave on the VME bus 28.

30   The sonar scanner 6, as shown in Figure 5 mounted separately on the measurement vehicle 40 in the pipe 42, includes a sonar head 100 which is based on a Simrad Mesotech Model 990 sonar system. The sonar head 100, as shown in Figure 6,

- 8 -

includes a transducer 102 for emitting sonar signals and receiving the return echoes 106, and a stepper motor 104 for rotating the transducer 102 at rates up to 2 revolutions per second. The sonar signals and echoes 106 therefore provide a circumferential scan 108 of the inner surface of the pipe 42 at each position z. The sonar head 100 further

5   includes a motor control circuit 105, a transmit/receive circuit 107, a signal processing circuit 110 and a general control circuit 112. The signal processing circuit 130 and the control circuit 112 are connected to the processing system 14 by the link 16, and the control circuit 112 on receiving a scan signal from the processing circuit 14 generates control signals for the motor control circuit 105 and the transmit/receive circuit 107 so

10   that the motor control circuit 105 begins controlling the motor 104 so as to rotate the transducer 102. The transmit/receive circuit 107 is then switched to transmit mode so as to cause the transducer to emit a short pulse of 2.2 MHz ultrasonic radiation and then reverts to receive mode so as to receive the sonar echo, which is passed to signal processing circuit 110 for transmission to processing system 14. A typical return ech

15   signal 114 is shown in Figure 7. The radial dimension r of the point on the scan 108 corresponding to the echo 114 is determined from the time between sending of the sonar pulse and the instant T 116 when the return signal level reaches a threshold level L 118, as discussed hereinafter. The second polar coordinate θ of the point on the scan 108 is determined from index pulses generated by the motor control circuit 106 for each

20   incremental step of the stepper motor 104, bearing in mind the initial orientation f the sonar transducer 102 is known. The pulses are transmitted to the processing system 14 from the motor control circuit 106 by the control circuit 112. Frequency multiplexing is used to provide separate channels with the processing system 14 for control signals to the head 100, and signals transmitted to the system 14. The analog signal 114

25   representing the intensity of the sonar echo as a function of time is digitised into 12-bit samples at a 250 kHz sampling rate using the A/D board 36 on receipt at the processing system 14. Prior to sampling, an 8-th order analogue low-pass filter with a cut-off frequency of 100 kHz is used to remove high-frequency components of the echo which may cause aliasing of the sampled signal. The output of the optical encoder of the

30   chainage detector 10 is obtained by the processing system 14 immediately after each sonar echo is received.

To determine the return time T of each sampled echo and from that the radial distance, r, to a feature of the inner surface of the pipe 42, three techniques are available, a curve–fitting technique, a cross–correlation technique, and a deconvolution technique. The curve–fitting technique involves fitting the echo samples to a curve for each echo

5   and then deriving the radial distance from the curve. The cross–correlation technique involves comparing the return samples with an echo from a known radius and using the cross–correlation result to determine the radial distance relative to the known radius.

The curve–fitting technique is performed as follows. A water to air interface is

10   an almost perfect mirror to sonar signals, and from an analysis of echoes obtained from a water–air interface using the transducer 102 it has been determined that a function of the form provided in equation (1) below can be used to describe a sonar echo produced by the sonar scanner 6.

$$y= \begin{cases} \sum c_i e^{-\lambda_i(t-\phi_i)^2}, & t \leq \phi_i \\ \sum c_i e^{-\lambda_i(t-\phi_i)^{\frac{3}{2}}}, & t > \phi_i \end{cases} \tag{1}$$

The parameters required to define each peak, i, of an echo, y, are the amplitude

15   of the peak, c_i, the width of the peak, λ_i, and the time at which the peak occurs, ϕ_i. The function y takes into account that the sonar signal generated by the transducer 102 has a trailing exponential decay at the end of the pulse. The derivative of the function y is discontinuous and the number of factors for each function is determined by the number of peaks detected in the return echo. A peak of the return echo is detected using an

20   estimate of the derivative of the samples of echo. A peak is defined to occur when there is a positive to negative zero–crossing of the derivative (indicating a change to the slope of the signal) and the height of the peak is greater than 5% of the maximum range of the samples, which eliminates for any noise inherent in the samples. Numerical differentiation is inherently a noise increasing operation, and to reduce noise components,

25   a five point smoothing differentiating filter, having a frequency response as shown in Figure 8, is used. The filter is implemented in software and the algorithm for implementing the filter is provided in equation (2).

– 10 –

$$y_k = \begin{cases} u_{k+1} - u_k, & 0 < k \le 2 \\ -0.08333u_{k+2} + 0.667u_{k+1} - 0.667u_{k-1} + 0.0833u_{k-2}, & 2 < k \le n-2 \\ u_k - u_{k-1}, & n-2 < k \le n \end{cases} \quad (2)$$

where u_k is the kth sample, y_k is the kth sample of the filtered signal and n is the number of samples.

An estimate of the time of the peak $\hat{\phi}_i$ is obtained by linear interpolation of the derivative values obtained on either side of the zero–crossing as shown in equation (3).

$$\hat{\phi}_i = \frac{\dot{y}_{i-1}t_i - \dot{y}_i t_{i-1}}{\dot{y}_{i-1} - \dot{y}_i} \quad (3)$$

The maximum value of the peak at $\hat{\phi}_i$ is estimated by fitting a quadratic through the three points prior and including the point after the zero–crossing of the derivative. An estimate of the width parameter λ_i is determined by locating the times of the half peak amplitudes on the rising and falling edges of a peak. Linear interpolation is again used between the two nearest sample values to the half amplitudes in order to obtain estimates of a time. The time difference between the peak and the half amplitude of the rising edge is used in preference to the falling edge, and if the time difference between the peak amplitude and half amplitude is given by w, then for the rising edge

$$\hat{\lambda}_i = \frac{-\ln(0.5)}{w^2} \quad (4)$$

and for the falling edge

$$\hat{\lambda}_i = \frac{-\ln(0.5)}{w^{\frac{3}{2}}} \quad (5)$$

After obtaining $\hat{\phi}_i$ and λ_i, c_i be solved for each peak using a matrix operation based on equation (1), which can give a least squares solution for c_i.

The echo return time or transit time T is determined to be time at which the function y for an echo reaches 10% of its maximum amplitude. The radial distance r_i

from the sonar head 102 to the internal feature of the pipe 42 that reflected the sonar signal to generate the echo is obtained by:

$$r_i = 0.5v_{sound}\left(\phi_i - \sqrt{\frac{-\ln(0.1)}{\lambda_i}} + t_{trig}\right) + r_{transducer} \qquad (6)$$

where v_{sound} is the velocity of the sonar signal; and ϕ_i and λ_i are the time and width parameters of the maximum peak of the echo. The time t_{trig} is the time between the start of emission of the sonar pulse and the time a trigger signal is received by the processing system 14 from the sonar head 100 and when the asynchronous sampling clock of the A/D board 36 begins sampling the echo. The signal processing circuit 110 of the head 100 generates the trigger signal at the end of generation of a sonar pulse. $R_{transducer}$ is half the width of the sonar transducer 102, which is approximately 10 mm.

The above solution for r_i can be performed in real−time using the microprocessor 38, or alternatively the work station 32 can be used and the initial parameter estimates for ϕ_i, λ_i and c_i fed to an fmins module of an algebra software package MATLAB to minimise the error between the fitted function y and the samples. An example of the results obtained for a three peak echo 120 is illustrated in Figure 9.

The cross−correlation technique first requires a standard sonar echo to be selected for cross−correlation with the echoes obtained in the pipe 42. A series of 10 echoes from an air/water interface were used to construct a standard echo template. The echoes were recorded using a cathode ray oscilloscope, at 8−bit resolution with a sample rate of 5 MHz and as there was a significant amount of switching noise and other signals, the echoes were averaged, the offset removed and the signal normalised. The template was digitally low−passed filtered using a 30 point filter with a cut−off frequency of 660 kHz. The leading signal of the standard peak is truncated so that the first point in the signal represents the beginning of the rise, which is the first part of the returning echo detected by the transducer 102. Therefore by truncating the standard signal in this manner the signal represents the shortest distance from the transducer 102 to a reflecting surface. The signal was then decimated according to the actual sampling period of the measured echoes to form the standard peak. The standard echo signal 122 is illustrated in

- 12 -

Figure 10.

A standard cross–correlation algorithm applied to a measured echo and the standard echo, is as follows:

$$R_{xy}(k) = \sum_{j=0}^{N-1} x(j)y(j+k), \quad -N + 1 \leq k \leq N - 1 \tag{7}$$

5   where:

x(k) is the measured sampled sonar echo,

y(k) is the standard sonar echo, and

$R_{xy}(k)$ is the cross–correlation of the vectors x(k) and y(k).

10   The location of the peaks of the cross–correlation are determined using equation (3), as discussed previously, and the location of the peaks gives the time lag between the standard and measured signals. An example of a typical cross–correlation 124 is shown in Figure 11. From the cross–correlation 124, the parameters ϕ_i and λ_i can be determined for the measured echo and the radial distance r_i determined using equation (6). The

15   cross–correlation method is significantly faster than the curve–fitting method when the latter uses the optimisation module fmins, however, the former method assumes that the return echo has the same profile as the standard echo.

An alternative technique for obtaining the parameters ϕ_i and λ_i for equation is to

20   apply a deconvolution algorithm, as follows, to the standard echo and the return echo.

$$S_{xy}(k) = DFT^{-1}\left\{\frac{Y*(f).X(f)}{Y*(f).Y(f)+s}\right\} \tag{8}$$

where

$$X(f) = DFT\{x(k)\} = \sum_{k=0}^{N-1} x(k)e^{\frac{-j2\pi fk}{N}}, \quad f = 0, \dots, N - 1,$$

is the discrete Fourier transform of the measured sampled sonar echo x(k),

$$DFT^{-1}\{X(f)\} = \frac{1}{N} \sum_{j=0}^{N-1} X(f)e^{\frac{j2\pi fk}{N}}, \; k = 0, \ldots, N-1,$$

is the inverse discrete Fourier transform of X(f),

$S_{xy}(k)$ is the signal resulting from the deconvolution of x(k) with y(k),

x(k) is the measured sample sonar echo,

y(k) is the standard sonar echo with discrete Fourier transform Y(f),

5   $Y^*(f)$ is the complex conjugate of Y(f), and

s is a small constant to prevent division by zero.

The accuracy of the raw ring data (x,y and r,θ data) for each position z obtained from the laser scanner 4 and sonar scanner 6, as discussed above, can be improved by
10 correction for movement of the measurement vehicle 40. The measurement vehicle 40 cannot be constrained to remain at the centre of the pipe 42 and orientated parallel with respect to the longitudinal axis of the pipe 42. Measurements obtained from the vehicle orientation detector 12 and the measured data can be used to determine components of motion of the measurement vehicle 40, such as x and y offsets from the centre of the pipe
15 42 to the prism 52 and the sonar head 102, and the yaw and pitch angles f the measurement vehicle 40. A method for correcting the raw data is discussed in the accompanying Appendix on pages 45 to 49, and involves obtaining the effects of the vehicle motion from the measured data and processing the measured data by a transformation required to transform a fitted ellipse onto a circle centred in the middle
20 of the pipe. The method assumes the pipe 42 is circular and first fits the ellipse t the ring data obtaining from the scanners 4 and 6. Having defined a fitted ellipse for the ring data, a transformation matrix is obtained which can be used to transform the ring data onto a circle corresponding to the assumed cross-section of the pipe 42. Defining the ellipse also provides offsets x_c, y_c to the centre of the pipe 42 which are used to correct
25 the cylindrical ring data so as to be centred on the centre of the pipe 42. The Appendix also describes how the yaw and pitch angles of the vehicle can be determined from the measured data and this can be used for comparison with signals obtained from a gyroscope of the vehicle orientation detector 12. The comparison enables adjustment of the measured yaw and pitch angles and calibration of the gyroscopes.

– 14 –

The plurality of ring data obtained over a length of the pipe 42 from the laser scanner 4 and the sonar scanner 6 each comprise a set of raw range data representing an image of the inner surface of the pipe which can be subjected to image processing. The range data comprises a set of z values, and for each value z is a plurality of x,y or r,θ

5   dimension values, corresponding to the features of the inner surface at each position z. All the x,y and r,θ values correspond to pixels of the image of the inner surface of the pipe 42.

The work station 32 first performs image preprocessing 200 on the range data 201

10   and then segments the pixels into regions of interest using an image segmentation procedure 202, as shown in Figure 12. The segmented regions are classified using a feed–forward neural network classifier of an image classification procedure 204. A classifier training procedure 206 trains the network classifier off–line using the back–propagation method. The classifier training procedure 206 relies on a training set

15   prepared by a preparation procedure 208. The training set preparation procedure 208 generates training data based on results obtained by performing the image segmentation procedure 202 on a known pipe structure with known defects. The results of the image classification procedure 204 are provided to an image interpretation procedure 208 which further defines the classified features of the image on the basis of a knowledge database

20   210 of known pipe features. A graphic display of the interpreted image can be produced at step 210 and an automatic defect report 212 produced at step 214, the reports generated being stored in a structured database 216.

The image preprocessing procedure 200 removes insignificant variations in the

25   range data and places it in a form which is not dependent on the type of scanner 4 or 6 used. The image preprocessing procedure 200 involves first processing the range data to produce a calibrated constant grid map of the internal surface of pipe 42, where the map is two dimensional and the surface of the pipe is considered to be split longitudinally and opened to expose the surface. The x,y and r,θ values for each pixel obtained by the

30   scanners 4 and 6 are calibrated and converted into depth values. Provision can also be made for pipe manufacturing tolerances. The depth value of each point on the grid map is determined by taking the depth value of the closest pixel to the point. Linear

interpolation can be used at an increased computational cost, but it has been found that the improvement gained does not justify the cost.

The image preprocessing procedure 200 involves generation of a pipe model, which represents a perfect pipe with no defects or features. The model provides a reference level with respect to which range or depth values can be measured.

Two techniques for data driven model generation have been implemented as part of the system 2. In each the first step is the identification of pixels in the image which are likely to be part of a defective region by differential geometric techniques.

Biquadratic surface patches are used to estimate image surface derivatives as described in "Surfaces in Range Image Understanding" by Paul J. Besl, Springer-Verlag, 1988. Pixels with small first derivatives may be called good pixels.

In the first model building technique the model is built ring by ring. An ellipse of best fit is determined for all the good pixels in a ring. The ellipse of best fit is obtained in the same fashion as discussed previously.

In the second model building technique the image is systematically covered with facets which are rectangular subimages. The facet with the largest number of good pixels is chosen. Multiple bilinear regression is carried out. If this is successful then the model is determined at that facet and the facet is "written" which means that all the pixel values in the facet are set to the values determined by the regression. If the regression is not successful then the facet is skipped and the best remaining facet is chosen. The regression will be successful if there are enough good pixels in the facet to get reliable results and the regression equations have a unique solution. Note that once a facet has "written" all its pixels become good.

After one pass through the facets in the image if there are any facets not written then the "read" size of the facets is incremented. This means that they examine pixels over a larger region when carrying out the regressions. When a regression for a facet is

- 16 -

successful it writes only to its initial region and not the extended read region. Successive passes are made in this way through the list of facets until all facets are written.

The advantage of the local facet method is that it applies to pipes of any shape.

The bilinear multiple regression for a facet is carried out by finding a facet or planar surface given by

$$f(x,y) = c + m_1 x + m_2 y,$$

which minimises

$$E(c, m_1, m_2) = \sum_i (f(x_i, y_i) - z_i)^2 = \sum_i (c + m_1 x_i + m_2 y_i - z_i)^2$$

Here z_i is the range value of the pixel (x_i, y_i) which is the ith good pixel in the rectangular subimage under consideration.

This minimum occurs with the vanishing of the following derivatives.

$$\frac{\partial E}{\partial c} = \sum_i 2(c + m_1 x_i + m_2 y_i - z_i)$$

$$\frac{\partial E}{\partial m_1} = \sum_i 2(c + m_1 x_i + m_2 y_i - z_i) \, x_i$$

$$\frac{\partial E}{\partial m_2} = \sum_i 2(c + m_1 x_i + m_2 y_i - z_i) \, y_i$$

This occurs when the following system of equations is satisfied.

$$nc + \sum_i x_i m_1 + \sum_i y_i m_2 = \sum_i z_i$$

$$\sum_i x_i c + \sum_i x_i^2 m_1 + \sum_i x_i y_i m_2 = \sum_i x_i z_i$$

$$\sum_i y_i c + \sum_i x_i y_i m_1 + \sum_i y_i^2 m_2 = \sum_i y_i z_i$$

This is a linear system and can be solved by standard methods.

The data of the laser scanner 4 usually has data values missing which may be

- 17 -

caused by a light absorbing surface, obstruction of the return light signal to the camera 56, a surface void, or surface which reflects light away from the camera 56. The missing values caused when an object obscures the line of sight between the camera 56 and the laser beam trace 55 are termed shadows. Symbolic values are assigned to all values

5 missing on the grid map. A set of possible values are obtained for the shadow pixels and other missing values by projecting a line from the camera position through every pixel. If any of these lines intersect the line projected from the centre of the pipe through the grid position of the missing value and perpendicular to the longitudinal axis of the pipe, the point of intersection is added to the set. Since this set of possible values is assumed

10 to be continuous only the minimum range value found need be kept for subsequent processing.

Shadows are not a considerable problem for the data obtained by the sonar scanner 6, however, instead of a single radial value for each point on the surface, there

15. may be several radial values caused by multiple echoes being returned to the sonar head 102. The sonar data is therefore further preprocessed by examination of the pixels in a window surrounding the current pixel, and a single depth value is chosen from amongst the pixel values in the window. The size of the window, presently 7×7, is dependent on the size of the area covered by the sonar signal 106 on the internal surface of the pipe

20 42.

The data obtained by both the laser scanner 4 and the sonar scanner 6 also contains a considerable amount of noise which can interfere with subsequent image analysis routines. The effects of the noise can be reduced by an image smoothing

25 process. An adaptive smoothing process is used for its properties of reducing noise whilst preserving discontinuities. An equally weighted local neighbourhood averaging kernal which adapts itself to the local topography of the surface to smooth is used. The resulting surface is smooth within regions whilst it's discontinuities (often corresponding to region boundaries) are preserved. The strategy consists of automatically selecting an

30 adequate kernal size which defines the size of the neighbourhood. The size of the smoothing kernal is based on an evaluation of the differences between the value at the centre point of the kernal window and its neighbours. The size of the kernal is chosen

such that the largest absolute difference between the centre pixel and it's neighbours is less than or equal to twice the noise level in the image and subject to the constraints that the kernal size is greater than a minimum size (typically 3 by 3) and smaller than a maximum size (typically 19 by 19).

5

The image segmentation procedure 202, as shown in Figure 13, includes a feature extraction step 220, a pixel labelling step 222 and a region extraction step 224. The feature extraction step 220 computes a set of features which are combined to form a feature vector for each pixel. The features used consist of features describing more or

10 less the range value properties of the pixel and features representing the texture in a local neighbourhood and include:

1.   The row r on the grid map for the pixel;
2.   The column c on the grid map for the pixel;
3.   The depth value f(r,c) of the pixel;

15 4.   The deviation from the Model f(r,c) − Model(r,c);
5.   First and second order derivatives of the function f at the position (r,c) based on estimating derivatives of digital surfaces as described in Besl; and
6.   Surface characteristics including biquadratic surface fit error, and quadratic variation as described in Besl.

20

The pixel labelling step 222 uses the feature vectors of the pixels to perform a classification technique which partitions the image into regions that are uniform with respect to certain features and that contrast with their adjacent neighbours in the same features. A Nearest Neighbour Classifier, which has been previously trained offline, is

25 used to perform the classification. The classifier is trained to classify pixels according to one of the following surface primitives:

background

void

30 corrosive

deposit

root

Training is performed by extracting a set of feature vectors from suitable known examples of the desired surface types. The set of feature vectors becomes the exemplar set for the classifier. The nearest neighbour classifier performs it's classification by comparing the unknown feature vector to it's set of exemplars. The assigned

5   classification is the same as the classification of the closest exemplar in feature space using the Euclidean distance measure. The output of the pixel labelling step 222 is a label list in the form of a function $l(r,c)$ which is the primitive surface classification for the pixel of row r in column c.

10 A relaxation step is used to improve the performance of the pixel labelling step. The underlying assumption of the relaxation process is that surface primitives consist of locally connected regions. This assumption is translated into the statement that classification decisions for single pixels are not independent of the decisions for neighbouring pixels. In other words, if all neighbours of a pixel are classified as pixels

15 of a certain primitive, it is very unlikely that this pixel does not belong to the same primitive. Since we want to modify the classification (label) at a pixel (r,c) we define a refined classification $l'(r,c)$ for the initial classification $l(r,c)$ as:

$$l'(r,c) = M (i,j \in Neighbourhood\ l(i,j))$$

Where neighbourhood is a certain neighbourhood (typically a 3 by 3 window) of (i,j) and M is a function of all the classifications in the neighbourhood of the pixel at

20 (i,j). Typically M is defined as the function returning the mode of it's arguments. The output of the relaxation step is a label list in the form of a function $l'(r,c)$ which is the refined primitive surface classification for the pixel of row r in column c.

The region extraction step 224 groups connected pixels having the same label into

25 connected components. Those connected components whose pixel type is not of the background type are extracted to form regions of interest R. The coordinates of a bounding rectangle for each region R is determined and a bit map, map(i,j), is generated to identify pixels of interest, i.e. those pixels within the region R belonging to the same connected component, where image :R $\rightarrow$ and bit map: R$\rightarrow$ {0,1}. The output of the

30 region extraction step 224 is a list of regions of interest in the range image of the pipe

- 20 -

surface.

        The image classification procedure 204, as shown in Figure 14, includes a filter
step 230, an interpolation step 232, a transform step 234 and a sampling step 336 which
5   process the bit maps of the regions of interest so as to place them in a form which can
be applied to the neural networks of a neural network classification procedure 238. The
output of the classification procedure 238 provides a classification for each region of
interest and a confidence value representative of the confidence that the classification is
correct. For example, classes for surface defects may include void, crack, corrosion or
10   deposit. The confidence value may be 0 or 1, i.e. low or high, or a "fuzzy" value
between 0 and 1.

        The neural networks used in the neural network classification procedure 238 have
a fixed structure, i.e. a fixed number of inputs and hidden layer nodes, yet the number
15   of pixels of interest in a region of interest and the size of the region is not fixed.
Therefore the data of the regions of interest must be manipulated so it can be applied to
the fixed inputs of the networks, regardless of region size, and this should be done
without sacrificing the data and true representation of the regions. This is achieved by
first applying a defect map filter at step 232 to the bit map of each region of interest.
20   The depth values for pixels of interest in the defect map are re-scaled to values between
1 and 2 and the remaining pixels are set to 0. This enhances the contrast between the
pixels of interest and the remaining pixels, highlights the boundary of a defect, while
retaining an image of the region's topography. The new image, image1, is defined for
all pixels(i,j) in the region R by equations (9), (10) and (11) below:

$$\text{image1}(i,j) = 0 \qquad\qquad (9)$$

25   for all (i,j) in R where map(i,j) = 0

$$\text{image1}(i,j) = f(\text{image}(i,j) - \text{model}(i,j)) \qquad (10)$$

for all (i,j) for which map(i,j) = 1 and the label represents an "outrusion", and

- 21 -

$$imagel(i,j) = g(model(i,j) - image(i,j)) \qquad (11)$$

for all (i,j) for which map(i,j) = 1 and the label represents an "intrusion". The functions f and g are given by, for example,

$$f(\delta) = 1 + \frac{\delta}{(\text{maximum radius} - \text{nominal radius})}$$

$$g(\delta) = 1 + \frac{\delta}{(\text{nominal radius} - \text{minimum radius})}$$

Nominal radius is that of the pipe, and maximum radius and minimum radius are the maximum and minimum depth or radius which the scanners 4 and 6 can detect.

5 Model(i,j) is the pipe model value at the pixel(i,j) where the pipe model can be obtained by either of the two methods described previously. The interpolation step 232 is used then to re-scale or compress the region of an arbitrary size m×n to an image, imag 2 : {0, ..., M-1} × {0, ..., N-1} → R, of a set size M×N so it can be applied to the neural networks. Transformation to the set image size is done by triangulation of the domain

10 of the region, which involves forming triangles with the vertices being the pixels of the region. The triangles have a number of different faces or "facets" orientated in different directions depending on the values of the pixels, and each triangle is then mapped to a function so as to form a continuous "facet" image. This image is then sampled onto a M×N grid to obtain the interpolated image. The form of the triangulation for a m×n

15 region is illustrated in Figure 15 where each grid is divided into an upper triangle 233 and a lower triangle 235. The continuous "facet" image is defined by a function f(x,y) where for any point (x,y) (0 ≤ x ≤ m-1 and 0 ≤ y ≤ n-1) in the grid map plane, f(x,y) is obtained by first finding the triangle which bounds (x,y). The triangle presents a facet in 3D space and f(x,y) is the height of the facet above the point (x,y). If (x_i, y_i) are the

20 vertices of a triangle (i = 1, 2 and 3) and z_i is the depth value corresponding to (x_i, y_i), then f(x,y) is evaluated as follows:

1.   If (x,y) lies in an upper triangle 233 then

$$f(x,y) = z_1 + (y - y_1 - x + x_1)(z_2 - z_1) + (x - x_1)(z_3 - z_1)$$

2.   If (x,y) lies in a lower triangle 235 then

- 22 -

$$f(x,y) = z_1 + (x - x_1 - y + y_1)(z_2 - z_1) + (y - y_1)(z_3 - z_1)$$

The function $f(x,y)$ is then sampled onto an M×N grid.

To reduce the data dimensionally further, the samples are transformed at step 234 from the spatial domain into a power domain or power spectrum using a discrete two dimensional Fourier transform. The power spectrum provides a good representation of the region due to the transformation process which reconstructs the surface in the Fourier domain. A discrete Fourier transform of image2 is performed using a recursive doubling strategy for Fast Fourier Transform (FFT). The discrete Fourier transform of an image $f : \{0, ..., M-1\} \times \{0, ..., N-1\} \rightarrow R$ is defined by equation (12).

$$F(u,v) = \sum_{k=0}^{M-1} \sum_{l=0}^{N-1} f(k,l) \exp\left(-i2\pi \left(\frac{ku}{M} + \frac{lv}{N}\right)\right), \tag{12}$$

k,l being the cartesian coordinates of image f and u,v being the cartesian coordinates of the transformed samples in the power domain, $0 \leq u, v \leq N-1$. The recursive doubling strategy is described in "Algorithms for Graphics and Image Processing" by Theo Pavlidis, Springer-Verlag, 1982. The power spectrum is the absolute value of the complex Fourier transform which gives a power domain image power : $\{0, ..., M-1\} \times \{0, ..., N-1\} \rightarrow R$, and $power(u,v) = | F(u,v) |$. The power spectrum is then wedge-ring sampled at step 236, which involves integrating, or summing, the samples in the power domain over eight wedge shaped and eight ring shaped sections of the domain. The result of the wedge-ring sampling provides a set of sixteen values which represent a compressed discrete signature of the inner surface of the pipe 42 which can be applied to the neural networks of the neural network classification step 238. The wedge-ring sampling is performed by first letting WEDGES be the number of wedges to be used and RINGS be the number of rings to be used. The interval from 0 to $\pi/2$ in the power domain is divided into WEDGES equal subintervals defined by angles $[\theta_i, \theta_{i+1}]$. The interval from 0 to $[(M-1)^2 + (N-1)^2]^{1/2}$ is divided into RINGS equal subintervals defined by radii $[r_j, r_{j+1}]$. The ith wedge sample is defined to be the sum of $power(u,v)$ for all (u,v) such that $theta(u,v)$ is in $[\theta_i, \theta_{i+1}]$ where theta : $R^2 \rightarrow [0, 2\pi]$ is the polar coordinate angle map given by

$$theta(u,v) = \arctan\left(\frac{v}{u}\right), \quad (u>0,v\geq0) \tag{13}$$

The jth ring sample is defined to be the sum of power(u,v) for all (u,v) such that radius(u,v) is in $[r_j,r_{j+1}]$ where radius : $R^2 \rightarrow [0,\infty]$ is the polar coordinate radius map given by

$$radius(u,v) = \sqrt{u^2 + v^2} \tag{14}$$

Thus, the ith wedge sample wedge(i) is defined by

$$wedge(i) = \sum_{k=0}^{M-1} \sum_{l=0}^{N-1} power(u,v)\, \chi_{[\theta_i,\theta_{i+1}]}(theta(u,v)), \tag{15}$$

5   and the jth sample ring(j) is defined to be

$$ring(j) = \sum_{k=0}^{M-1} \sum_{l=0}^{N-1} power(u,v)\, \chi_{[r_j,r_{j+1}]}(radius(u,v)), \tag{16}$$

where for any wedge or ring set S, χ_s is the characteristic function of S which indicates whether x, being theta(u,v) or radius (u,v), is in S, and is defined by

$$\chi_s = \begin{cases} 1 & \text{if } x \in S \\ 0 & \text{if } x \notin S \end{cases} \tag{17}$$

The wedge–ring samples are put together to form a feature vector. The first WEDGES, in this case eight, features are the wedge samples and the last RINGS, in this case eight,
10   features are the ring samples.

The Fourier transform and wedge–ring sampling steps 234 and 236 preserve the overall shape and texture of the regions of interest and enables the neural network classifier to discriminate between complex surface defects. A number of factors enable
15   this to occur, as discussed above, and are a consequence of the fact that the Fourier transform is an invertible mapping onto the frequency domain, and the power spectrum is translation invariant, which ensures the wedge–ring samples are translation invariant. Furthermore, the wedge samples are scale invariant and the ring samples are rotation invariant. This facilitates invariant classification of defects in the pipe surface.

- 24 -

The neural network classification step 238 involves applying the wedge–ring samples to a number of feed–forward neural networks which have been trained by the back–propagation method. A neural network 241, as shown in Figure 16, is provided for each classification class of surface defects and pipe features. The networks 241 each

5   presently have a topology of 16 inputs 243 in the input layer 239, eight nodes 235 in the first hidden layer 247, four nodes 249 in the second hidden layer 251 and two outputs 253 in the final fourth layer 255. Weights $W_\ell(i,j)$ are applied to each value passed between the four layers 239, 247, 251, 255, ℓ being the layer number, i being the number of the node or output of the layer ℓ and j being the number of the node or input of the

10   $\ell+1$ layer. Biases are applied to the result of summing all of the weighted values received at each node 245 and 249. The outputs include one for an affirmative signal, and one for a negative signal, the signal level being between 0 and 1 on each output and indicating a degree to which the network believes the region of interest belongs to its respective class or not.

15

The neural networks are divided into a first class which operates on images that represent intrusions into the pipe, and the second class which operates on images that represent defects or features that protrude away from the centre of the pipe 42. An example of the first class is the tree root/non–tree root neural network classifier, and its

20   weights and biases are listed below in natural order below, the weights for each node being provided first, starting from the first input 243 of the first layer 239 to the outputs of the fourth node 249 of the third layer 251, and the biases of the nodes 247 and 249 being specified thereafter.

25   12.746346 0.645722 2.463586 5.257362 –0.197740 8.822066 0.945439 2.853589
     0.449587 1.397464 –0.533578 5.705785 1.628069 –1.967862 –0.239797 –0.373825
     1.377219 0.520709 0.453015 4.017916 0.673481 –0.234437 0.156330 0.080759 3.560530
     0.024726 1.190002 –0.358105 0.618113 3.074333 0.747060 1.033451 3.579981 0.893241
     –0.071298 4.316509 1.267015 1.493471 0.237219 0.511365 2.099212 1.018908 1.023318
30   1.529006 0.670844 1.240182 0.540520 0.775410 –0.014260 1.262444 –0.958270
     6.563632 1.846852 –2.157752 0.372251 –0.693959 –3.006805 1.458163 –1.210690
     7.822542 2.175437 –4.379960 –0.061603 –1.556301 –26.296545 2.685686 –10.934907

11.470201 5.980796 −28.453907 −4.285449 −11.180037 2.963111 0.922024 0.107060
3.644659 0.804294 1.390882 0.702610 0.869146 1.932907 1.144155 0.490662 2.916481
0.284488 0.304954 0.552635 0.230630 2.314049 0.639178 −0.134080 3.930335 0.525155
0.944172 0.529907 −0.047074 7.097008 0.538283 2.110033 0.402595 −0.196998
5.534210 1.178307 2.593368 2.963713 1.239985 −0.773600 12.584067 1.767470
−1.303928 −0.271549 −0.504803 0.201155 1.116746 −0.746619 6.032501 2.042504
−2.044746 −0.043633 −1.141010 −1.374343 0.919341 −1.191014 7.024599 1.851477
−3.833785 −0.535100 −1.051623 −2.154537 −1.302927 −1.167616 −14.931460
−0.376227 −0.283871 −0.052614 3.021743 0.684641 −1.029852 −0.681440 −5.504961
2.518857 −0.470717 0.093677 18.494614 0.617955 −0.325076 0.309436 5.028311
−1.376231 −2.193236 −1.027059 −14.613549 0.687801 −0.960444 −0.916111 −2.058457
−0.389501 −1.347371 −0.341156 −5.834723 −1.902474 1.838991 0.517196 −0.478243
0.028812 0.223330 3.593781 −3.583304 −1.741506 1.305033 −0.042125 6.244700
0.438302 −2.012424 1.386442 −0.002000 −1.619284 1.642677 2.030912 −12.951331
0.616731 −0.642265

An example of the second class of neural network is the pipe join/non pipe join neural network classifier, the weights and biases of which are listed below in natural order.

15.601082 1.313890 −4.911501 2.071737 6.847770 −1.955913 0.479759 23.305962
−11.033848 0.294237 −9.093491 1.763276 13.544494 −9.255530 −0.530280 −12.524919
−6.430345 −0.506124 1.793031 0.236400 11.959572 8.719585 0.085171 −10.598364
14.464748 0.104221 18.004253 −2.007996 −7.571867 37.566628 1.563560 9.753113
3.913759 0.088835 2.713513 0.757766 23.501945 18.608824 0.587159 1.179299
−11.030748 0.242176 −5.094967 0.842696 15.003055 −2.304438 −0.025316 −14.214068
−14.926097 0.035510 −11.846221 1.631934 28.704191 −10.829489 0.083905 −16.000715
−15.083493 0.116805 −5.290942 0.712775 16.129330 −8.731529 −0.287789 −17.385916
24.353518 1.897373 3.986410 1.951551 15.928616 5.156585 1.666751 32.937801
3.532454 0.609612 −1.327396 1.226175 3.727180 1.971728 0.745650 4.040071 1.858634
0.535590 2.401938 0.487294 −0.504847 9.046494 0.441551 0.203021 −18.910927
−0.660695 −8.226106 1.381131 12.661963 −7.653401 −0.483721 −24.692900 10.056084

0.513577 6.766282 0.206353 0.355041 22.668598 1.356813 8.777742 –1.936229

–0.228150 6.818745 0.594466 30.175247 23.757566 0.693519 –7.394564 –7.025899

–0.038548 –6.210098 1.386558 13.0933873 –3.644164 –0.309244 –8.490670 –21.163414

–0.423117 –17.802017 2.518166 33.727161 –24.713118 –1.424613 –21.156178

5   –8.455983 0.184931 0.430795 –12.507034 –1.018161 –0.215443 –0.097470 –0.057819

9.579165 –0.587254 –0.855436 –12.936895 –1.489346 –0.738745 –0.257254 2.980933

17.244980 3.112999 –1.679418 33.106018 13.431716 –3.643328 –2.187083 –24.992414

0.823561 –0.437280 –0.970514 –1.308472 –16.635191 –2.442617 2.454849 –9.283930

2.711961 –2.711932 0.368954 –0.368977 –0.886622 0.886741 –2.976039 2.976049

10   4.088806 3.415415 –0.099539 2.509209 15.089481 5.665998 3.394832 5.804759

–6.528076 –1.664564 2.117919 –19.312078 1.332425 –1.332394

The weights and biases for the neural networks are established by the classifier training procedure 206 which uses the back–propagation method, as discussed in "Neural

15   Computing" by R. Beale and T. Jackson, IOP Publishing 1990, on a data set prepared by the training set preparation procedure 208. This involves obtaining data on known pipe defects and features using the pipe inspection system 2 and then on segmentation of the data by the segmentation procedure 202 providing the results to the preparation procedure 206 which performs the filtering, interpolation, Fourier transform and wedge–ring

20   sampling steps 230 to 236 to create the data sets. The data sets together with their known classification results are fed to the classifier training procedure 206 which attempts to seek convergence of the weights and biases using the back–propagation method to produce correct neural networks for each classification class. The data sets are randomly interleaved, i.e. for the tree root network, the tree root data sets are interleaved with data

25   sets that do not relate to tree roots so as to obtain accurate convergence of the weight and bias values.

Filters are used with some of the dedicated networks. For example, with the pipe–connection network if the bounding rectangle length of the region of interest is less

30   than i_FILTER or the bounding rectangle height is less than j_FILTER or the defect map area is less than area_FILTER then "not pipe join" is returned and use of the neural network is circumvented.

- 27 -

The image interpretation procedure 208 involves the verification and rating of each classified region of interest based on a database of 210 of defect and pipe feature characteristics and previously identified defects and features, which includes defect characteristics, e.g. direction/angle, gradient, area, and depth of defects, ratings, e.g.

5   structural, service or other, and spatial relation with other defects or features. The image interpretation procedure 208 is separated into two parts, as shown in Figure 17, an image analysis step 250 which performs further image analysis on the bit maps of the classified regions in order to determine additional feature attributes associated with the pixels of interest, at step 252. The feature attributes may include direction, edge details, area,

10   position and depth of a surface feature or defect. An inference engine step 254 is provided to match the model of the defects provided in the knowledge database 210 using a set of defect identification and rating rules 256 which may be coded in an "if condition then conclusion" format. The inference engine is a general purpose facility. The application dependent interface functions are provided to interface between the engine and

15   the application program's data.

The image interpretation procedure 208 is supported by other procedures for the efficient application of a knowledge base. These are:

20   •   **Rule base maintenance** provides facilities for the addition, modification and deletion of rules from a knowledge base.

•   **Rule base compiler** parses the knowledge base and ensures correct syntax. The knowledge base is then translated into a format suitable for the knowledge base

25   engine.

The following specifies the knowledge base for complete identification of the service and structural defects and features.

30

– 28 –

SERVICE AND STRUCTURAL DEFECT SCORING RULES

Grease

    IF   region is grease

5   AND

           cross–sectional area loss is less than 5%

    THEN

        score is 1.0 * length(m)

10 IF   region is grease

       AND

           cross–sectional area loss is not less than 5%

       AND

           cross–sectional area loss is less than 20%

15 THEN

        score is 5.0 * length(m)

Roots

    IF   region is a root

20   AND

           cross–sectional area loss is less than 5%

    THEN

        score is 2.0

25 IF   region is root

       AND

           cross–sectional area loss is not less than 20%

    THEN

        score is 5.0

30

    Note: Root scoring varies slightly from Australian Conduit Condition Manual

Open Joints

IE   region is an open joint

        AND

                'openness' is less than the pipe wall thickness

5   THEN

        score is 0.1

IE   region is an open joint

        AND

10   'openness' is greater than the pipe wall thickness

        AND

                'openness' is less than 1.5 pipe wall thicknesses

THEN

        score is 2.0

15

Displaced Joints

IE   region is a displaced joint

        AND

                displacement is less than the pipe wall thickness

20 THEN

        score is 0.1

IE   region is a displaced joint

        AND

25   displacement is greater than the pipe wall thickness

        AND

                displacement is less than 1.5 pipe wall thicknesses

THEN

        score is 0.5

30

IE   region is a displaced joint

        AND

– 30 –

displacement is greater than 1.5 pipe wall thicknesses

THEN

score is 2.0

5　**Encrustation**

IF　region is encrustation

AND

cross–sectional area loss is less than 5%

THEN

10　score is 1.0 * length(m)

IF　region is encrustation

AND

cross–sectional area loss is not less than 5%

15　AND

cross–sectional area loss is less than 20%

THEN

score is 2.0 * length(m)

20　IF　region is encrustation

AND

cross–sectional area loss is not less than 20%

THEN

score is 5.0 * length(m)

25

Scale

IF　region is scale

AND

cross–sectional area loss is not less than 5%

30　THEN

score is 1.0　length(m)

      IF   region is scale

      AND

           cross-sectional area loss is not less than 5%

      AND

5   cross-sectional area loss is less than 20%

  THEN

      score is 2.0 * length(m)

      IF   region is scale

10   AND

           cross-sectional area loss is not less than 20%

  THEN

      score is 5.0 * length(m)

15 **Cracked**

      IF   region is a circumferential crack

  THEN

      score is 1.0 * length(m)

20 IF   region is a longitudinal crack

  THEN

      score is 2.0 * length(m)

      IF   region is a multiple crack

25 THEN

      score is 5.0 * length(m)

  Fractured

      IF   region is a circumferential fracture

30 THEN

      score is 8.0 * length(m)

IF   region is a longitudinal fracture
THEN

      score is 15.0 * length(m)

5 IF   region is a multiple fracture
THEN

      score is 40.0 * length(m)

Gas Attack

10 IF   region is gas attack
     AND

         extent is slight
THEN

      score is 2.0 * length(m)

15

    IF   region is gas attack
     AND

         extent is medium
THEN

20   score is 40.0 * length(m)

    IF   region is gas attack
     AND

         extent is extreme
25 THEN

      score is 100.0 * length(m)

Erosion

    IF   region is erosion
30   AND

         extent of slight
THEN

– 33 –

score is 1.0 * length(m)

IF   region is erosion
        AND
5   extent is medium
THEN
        score is 25.0 * length(m)

IF   region is erosion
10   AND
                extent is large
THEN
        score is 100.0 * length(m)

15 **Deformed**
    IF   region is deformed
          AND
                  deformation is less than 10%
    THEN
20   score is 10.0 * length(m)

    IF   region is deformed
          AND
                  deformation is not less than 10%
25   AND
                  deformation is less than 15%
    THEN
          score is 30.0 * length(m)

30 IF   region is deformed
          AND
                  deformation is not less than 15%

AND

deformation is less than 20%

THEN

score is 90.0 * length(m)

5

IF   region is deformed
        AND

deformation is not less than 20%
        AND

10   deformation is less than 25%

THEN

score is 125.0 * length(m)

IF   region is deformed
15   AND

deformation is not less than 25%

THEN

score is 165.0 * length(m)

20 **Broken**
    IF   region is broken
    THEN

score is 60.0

25   The image interpretation procedure 208 allows the defects and pipe features
specified in the following tables to be identified. The tables specify the neural network
classification given to the defects and features, and feature attributes which need to be
determined by the image analysis step 250 in order for the inference engine step 254 to
complete identification of the defects and features.

30

            The tables document the attributes used by the rule base to classify regions. A
tick indicates that the region should strongly exhibit this attribute whilst a cross indicates

that the region should not exhibit this attribute. A dash indicates a don't care situation. The tables do not indicate whether the attributes are used in the conjunctive or disjunctive manner.

Classification	Attributes												
	Smooth Corrosion	Rough Corrosion	Void	Pipe Connect.	Smooth Deposit	Rough Deposit	Roots	Area Loss < 5%	Area Loss < 20%	Area Loss >= 20%	Axis Orientam. Parallel	Centroid Position Crown	Extensive
Light Encrustation	x	x	x	x	✓	x	x	✓	x	x	-	-	x
Medium Encrustation	x	x	x	x	✓	x	x	x	✓	x	-	-	x
Heavy Encrustation	x	x	x	x	✓	x	x	x	x	✓	-	-	x
Light Scale	x	x	x	x	x	✓	x	✓	x	x	-	✓	✓
Medium Scale	x	x	x	x	x	✓	x	x	✓	x	-	✓	✓
Heavy Scale	x	x	x	x	x	✓	x	x	x	✓	-	✓	✓
Light Grease	x	x	x	x	✓	x	x	✓	x	x	-	-	✓
Medium Grease	x	x	x	x	✓	x	x	x	✓	x	-	-	✓
Heavy Grease	x	x	x	x	✓	x	x	x	x	✓	-	-	✓
Fine Roots	x	x	x	x	x	x	✓	-	-	-	-	-	-
Tap Roots	x	x	x	x	x	x	✓	-	-	-	-	-	-
Light Root Mass	x	x	x	x	x	✓	✓	✓	x	x	-	-	x
Medium Root Mass	x	x	x	x	x	✓	✓	x	✓	x	-	-	x
Heavy Root Mass	x	x	x	x	x	✓	✓	x	x	✓	-	-	x

Classification	Smooth Corrosion	Rough Corrosion	Void	Pipe Connect.	Smooth Deposit	Rough Deposit	Roots	Crackness	Complex	Maximum Deviation > 'ι'	Axis Orientatn. Parallel	Centroid Position Crown
Circumferential Crack	✓	✓	✓	x	x	x	x	✓	x	x	x	-
Longitudinal Crack	✓	✓	✓	x	x	x	x	✓	x	x	✓	-
Multiple Crack	✓	✓	✓	x	x	x	x	✓	✓	x	-	-
Circumferential Fracture	✓	✓	✓	x	x	x	x	✓	x	✓	x	-
Longitudinal Fracture	✓	✓	✓	x	x	x	x	✓	x	✓	✓	-
Multiple Fracture	✓	✓	✓	x	x	x	x	✓	✓	✓	-	-
Slight Gas Attack	✓	x	x	x	x	x	x	x	-	-	-	✓
Medium Gas Attack	x	✓	x	x	x	x	x	x	-	x	-	✓
Large Gas Attack	x	✓	x	x	x	x	x	x	-	✓	-	✓
Extreme Gas Attack	x	✓	x	x	x	x	x	x	-	✓	-	✓
Slight Erosion	✓	x	x	x	x	x	x	x	-	-	-	x
Medium Erosion	x	✓	x	x	x	x	x	x	-	x	-	x
Large Erosion	x	✓	x	x	x	x	x	x	-	✓	-	x
Broken	x	x	✓	x	x	x	x	x	-	-	-	-

Attributes

- 38 -

The pipe position in rings, clock reference, and the pixels of the regions of interest corresponding to each defect and feature identify the precise location of a defect or feature. The rules 256 can also be used to resolve location conflicts which may occur during segmentation and classification when different defects overlap. At least three
5   different types of conflicts can be resolved, conflicts among superimposed defects, conflicts among adjacent defects, and conflicts arising due to classification ambiguities between different parts of defects.

The use of the knowledge based interpretation procedure 208 after the
10   segmentation and classification procedures 202 and 204 enhances the identification and detection of surface defects. Furthermore, the database 210 enables the severity of the defects to be evaluated and rated, from which a comprehensive report can be generated using the report generation procedure 214.

15   The report is outputted in the following form:

Distance Rings	Condition Code	Dia/Dim Clock at to	%	Remarks
1	SES	0103		Surface Erosion Slight
6	SES	0303		Surface Erosion Slight
29	SES	0203		Surface Erosion Slight
36	SES	0203		Surface Erosion Slight
49	EL	0506	00.07	Encrustation Light
42	SES	0102		Surface Erosion Slight
52	SES	0204		Surface Erosion Slight
66	EL	0607	00.08	Encrustation Light
92	EL	0204	01.30	Encrustation Light
108	EL	0608	01.45	Encrustation Light
184	EL	0608	00.75	Encrustation Light
248	SES	0202		Surface Erosion Slight
269	EL	0708	00.27	Encrustation Light
252	RF	0609	05.18	Fine Tree Roots
276	B	0708		Broken
321	B	1204		Broken
498	SES	0708		Surface Erosion Slight

539	EL	0709	01.75	Encrustation Light
555	B	0709		Broken
752	SES	0405		Surface Erosion Slight
805	JNT	0411		Pipe Joint
817	CL	0304		Longitudinal Crack
835	RF	0506	00.29	Fine Tree Roots
867	SES	0405		Surface Erosion Slight
841	EL	0405	00.92	Encrustation Light
856	CL	0102		Longitudinal Crack
879	RF	0305	01.61	Fine Tree Roots
874	EL	0306	01.15	Encrustation Light
906	B	0405		Broken
919	EL	0507	00.79	Encrustation Light
945	EL	0507	00.56	Encrustation Light
971	EL	0609	00.97	Encrustation Light
962	RF	0709	04.13	Fine Tree Roots
980	B	0709		Broken
976	EL	0405	00.73	Encrustation Light
1035	SES	0808		Surface Erosion Slight
1096	EL	0306	01.05	Encrustation Light
1101	EL	0810	01.09	Encrustation Light
1157	JNT	0605		Pipe Joint
1191	EL	0303	00.02	Encrustation Light
1172	B	1105		Broken
1178	B	0102		Broken

In order to allow further evaluation of defect severity, and to provide information about changes in pipe condition, a Management Information System (MIS) has been developed. It uses the work station 32 to provide a graphic user interface (GUI) which allow the asset manager or engineer to call up selected previously processed data sets, and to interactively display the defect regions, or to generate new reports using a modified rulebase. The MIS has been written to run in a main window of the display 211. The main window will list the assessment for each of the defects, and allows display of multiple detailed views of the data related to the defect. These alternate views can comprise: one showing the current ring slice of the pipe data, one showing the

– 40 –

current range or unwrapped section of the pipe data, and the other showing a three dimensional (3D) display of the pipe data. The MIS can also provide a graph showing variation of rating over time, based on previous pipe inspections.

5   The MIS has been designed and implemented in a modular fashion, and Figure 4 shows the main MIS software components.

Through the MIS, the user (such as an asset manager or maintenance engineer), can control access to the data base using the GUI. The GUI sub-system allows the user
10   to specify the operation (either data interpretation, visualisation or comparison) and the data to operate on (either the entire list of regions of interest, or a subset of it). The GUI sub-system invokes the sub-system which performs the particular operation on the data requested by the user. The called sub-system loads the specified data from data base using the facilities provided by the interfacing sub-system, if it has not been previously
15   loaded. When the analysis sub-system is called, it in turn calls components from the knowledge base sub-system, to apply the knowledge base(s) to the data. A default knowledge base(s) is used except where the user explicitly overrides this default through the user interface.

20   The graphical user interface (GUI) processes interactive user requests that are activated using the keyboard and mouse. The GUI provides menus and windows to enable easy interaction with the system. It contains the control logic to sequence and control the interaction with, and of, the sub-systems.

25 The GUI provides access to, or invokes facilities for:

        Data load
        Data save
        Knowledge base maintenance
30   Pipe analysis
        Comparison over time
        Compare two analyses

– 41 –

Visualise an analysis

The software uses a computer graphics display to provide visualisation of analysed lists of regions of interest. Various views can be generated depending on a viewing
5 position and data supplied by the GUI sub–system. That is, when the viewing parameters are changed in the GUI, the views are automatically regenerated to reflect this change. This sub–system provides display services to the other sub–systems.

The visualisation sub–system generates a required picture from the supplied data,
10 scales the picture to the appropriate window size and draws the picture into a graphics window.

The following services are provided by this sub–system:

15 • **Cross section view** generates a cross–sectional view of the pipe taken at the nominated pipe position. The generated image is scaled appropriately to fill the viewing window.

• **Unwrapped view** generates an unwrapped view of the pipe starting at the
20 nominated pipe position.

• **3D view** generates a 3D perspective view of the pipe from the nominated pipe position. The orientation of the viewing camera is provided to enable the generation of the view from almost any position. The generated image is scaled
25 appropriately to fill the viewing window.

• **Graphing** produces a 2D line graph from the two data vector parameters.

A comparison sub–system relates multiple pipe condition assessment results. A
30 time–based rating of assessment results can be assembled and displayed as a graph.

The following is an example of the service provided by this sub–system:

– 42 –

- **Comparison over time** examines all analysed lists of regions of interest for a given pipe and for each list extract and time stamp the assessment rating.

An interfacing sub–system provides a level of abstraction between the system and the underlying operating system and any external systems that require interfacing to. This subsystem is intended to provide a library of interfacing services (which are implementation, or organisation, specific).

The following services are provided by this sub–system:

- **Data load** reads data from the supporting file system and converts it into a form suitable for the internal set of regions structure.

- **Data save** extracts data from the internal set of regions of interest and converts it into a form suitable for writing to the underlying file system.

- **Pipe directory** interrogates the file system and returns the set of all pipe identifiers.

- **Analysis directory** interrogates the file system and returns the set of all analysis identifiers for a given pipe.

- **Analysis export** extracts information from the results of the analysis and formats the data in a form suitable for import into Water Authority databases.

- **Printing** displays results on a printer device.

The data managed by the MIS system is primarily made up of *list of regions of interest* information for a pre–processed *pipe image*. The information stored in, or calculated for, each region of interest consists of region attributes which include: region location in the pipe; an image of the region, a region type descriptor, a region classification, area, perimeter, cross–sectional area loss, geometric descriptors, rating, etc.

The list of regions of interest encapsulates the information used for condition assessment from the raw sensor pipe data. This list of regions of interest is a main data component within the system 2 and it is extensively used by both the analysis and comparison subsystems via an interfacing sub-system.

5

The *pipe image is* a form of annotated grid of pixel values representing a pipe surface in 3D space.

The *list of regions of interest* contains attribute and sub-image information for
10   each segmented region.

A knowledge base representation is another data structure, which is an internal representation of an ASCII file of structured English-like declarative rules and functions.

15   *Raw pipe* data from the sensors is supplied to the pre-processing module in real-time or as a file. After pre-processing and compression the *pipe image* data is transformed into a *list of regions of interest* and put into the data base. This data base can be archived or input directly into MIS to perform pipe analysis. For a given pipe there may be many *lists of regions of interest*, each one corresponding to a particular run
20   of a given sensor through the pipe.

The interfacing sub-system provides an abstract conduit between the data used by the MIS and the data base structure within the underlying operating system, as well as *external data bases* to which the user required information about the list of regions of
25   interest may be sent to, or retrieved from.

Assessment rules are input from the user into a knowledge base representation used by the knowledge base sub-system with a text editor. The knowledge base representation can also be compiled directly into the knowledge base sub-system.
30

The implementation of the graphical user interface (GUI) assumes the availability of a mouse and a colour graphical display. The MIS is designed to be interactive, and

a user is required at most stages of MIS processing. However, most analysis actions of the system 2 can be performed, if desired, in a batch mode (i.e. without user intervention).

5   The MIS can be operated independent of the data collection device, in a office environment using an appropriately configured and fast Sun Microsystem's Sparc 10 workstation. The recommended initial configuration of the workstation is:

          Single or dual CPU SPARC 10 Mbus module
10   32 MB or more in parity SIMMS
          SCSI-2 controller
          1.05GB fast internal SCSI-2 hard disk
          19" colour display capable of 1280x1024 resolution
          Industry standard keyboard and mouse
15   IEEE 802.3 Ethernet and serial ports
          150MB 1/4" Desktop Tape Drive
          pre-installed: Solaris 2.x, SPARC Compiler C++, Motif Toolkit

          A simplified interface to gather and pre-process raw sensor data can be run on
20   a minimally configured Sparc workstation installed in a field environment. The transport of data from the field to the office workstation can be via magnetic tape. The recommended initial configuration is:

          Single CPU SPARC 2 Sbus module
25   32 MB or more in parity SIMMS
          SCSI-1 controller
          424 MB internal SCSI-1 hard disk
          19" colour display capable of 1280x1024 resolution
          Industry standard keyboard and mouse
30   IEEE 802.3 Ethernet and serial ports
          150MB 1/4" Desktop Tape Drive
          pre-installed: Solaris 1.x, XGL Graphics Software

Appendix: Vehicle motion correction

1   Introduction

Data from both laser and sonar scanners is processed into the form of cylindrical coordinates (r, θ, z). This data can be corrected for movement of the vehicle relative to the pipe axis. This can improve measurement accuracy as the vehicle may not remain at the center of the pipe and oriented parallel with the pipe's longitudinal axis.

There are two methods to determine the required corrections:

1. measure the motion using sensors, or

2. use the measured data to estimate the motion of the vehicle.

A combination of these two methods is utilised, with sensors being used to measure some of the motions and the measured data being used to obtain the others.

Figure 18 shows the orientation detector 12 at an arbitrary orientation and position in the pipe. The orientation of the vehicle can be described by roll, pitch and yaw angles (θ, ϕ, ψ), while (x, y, z) coordinates can be used to describe its position.

2   Ellipse fitting method

The following steps are undertaken to remove the effects of vehicle motion from measurements:

1. the data is transformed into Cartesian coordinates using:

$$x_i = r_i \cos \theta_i \qquad (1)$$
$$y_i = r_i \sin \theta_i, \qquad (2)$$

2. an inclusion zone is estimated from the orientation and radius of the previous point; all data not in this region is excluded from the estimator so as not to bias the estimates with the defects in the pipe,

3. an ellipse is fitted to the included data using algorithms outlined below,

4. the data is corrected for rotational misalignment and x- and y-axis translations,

5. the data is transformed data back into cylindrical coordinates using

$$\tan \theta_i = \frac{y_i}{x_i} \qquad , \qquad (3)$$
$$r_i = \frac{x_i}{\cos \theta_i} = \frac{y_i}{\sin \theta_i}. \qquad (4)$$

The equation of a conic section can be expressed as:

$$x^2 + w_1 y^2 + w_2 xy + w_3 x + w_4 y + w_5 = 0 \qquad (5)$$

A general ellipse with center (x_c, y_c), major and minor axes of a and b respectively, rotated through γ radians from the x-axis is shown in Figure 19.

The equation for the ellipse in the (x, y) coordinate frame can be determined by suitable transformations from the equation of the ellipse in the (x'', y'') coordinate frame,

$$\left(\frac{x''}{a}\right)^2 + \left(\frac{y''}{b}\right)^2 = 1.$$

Using the transformations:

$$\left[\begin{array}{c} x' \\ y' \end{array}\right] = \left[\begin{array}{cc} \cos\gamma & \sin\gamma \\ -\sin\gamma & \cos\gamma \end{array}\right]\left[\begin{array}{c} x'' \\ y'' \end{array}\right]$$

and

$$\left[\begin{array}{c} x \\ y \end{array}\right] = \left[\begin{array}{c} x' \\ y' \end{array}\right] - \left[\begin{array}{c} x_c \\ y_c \end{array}\right]$$

yields the following equation for the ellipse in the (x, y) coordinate frame:

$$
\begin{aligned}
&\left(b^2\cos^2\gamma + a^2\sin^2\gamma\right)x^2 + \left(b^2\sin^2\gamma + a^2\cos^2\gamma\right)y^2 - \\
&\qquad 2\left(b^2\cos\gamma\sin\gamma - a^2\cos\gamma\sin\gamma\right)xy + \\
&\left(-2x_c\left(b^2\cos^2\gamma + a^2\sin^2\gamma\right) + 2y_c\left(a^2\cos\gamma\sin\gamma - b^2\cos\gamma\sin\gamma\right)\right)x + \\
&\left(2x_c\left(a^2\cos\gamma\sin\gamma - b^2\cos\gamma\sin\gamma\right) - 2y_c\left(b^2\sin^2\gamma + a^2\cos^2\gamma\right)\right)y + \\
&\left(b^2\cos^2\gamma + a^2\sin^2\gamma\right)x_c^2 + \left(b^2\sin^2\gamma + a^2\cos^2\gamma\right)y_c^2 + \\
&\qquad 2\left(b^2\cos\gamma\sin\gamma - a^2\cos\gamma\sin\gamma\right)x_c\,y_c + a^2b^2 = 0
\end{aligned}
\tag{6}
$$

Equating the coefficients of Equation 6 to those in Equation 5 results in the following equations for the w_i.

$$w_1 = \frac{\left(b^2\sin^2\gamma + a^2\cos^2\gamma\right)}{\left(b^2\cos^2\gamma + a^2\sin^2\gamma\right)} \tag{7}$$

$$w_2 = \frac{2\left(b^2\cos\gamma\sin\gamma - a^2\cos\gamma\sin\gamma\right)}{\left(b^2\cos^2\gamma + a^2\sin^2\gamma\right)}$$

$$w_3 = \frac{-2\left(b^2\cos^2\gamma + a^2\sin^2\gamma\right)x_c + 2\left(b^2 - a^2\right)\cos\gamma\sin\gamma y_c}{\left(b^2\cos^2\gamma + a^2\sin^2\gamma\right)}$$

$$w_4 = \frac{-2\left(b^2 - a^2\right)\cos\gamma\sin\gamma x_c - 2\left(b^2\sin^2\gamma + a^2\cos^2\gamma\right)y_c}{\left(b^2\cos^2\gamma + a^2\sin^2\gamma\right)}$$

$$w_5 = \frac{\left(b^2\cos^2\gamma + a^2\sin^2\gamma\right)x_c^2 + 2\left(b^2 - a^2\right)\cos\gamma\sin\gamma x_c\,y_c + \left(b^2\sin^2\gamma + a^2\cos^2\gamma\right)y_c^2 - a^2b^2}{\left(b^2\cos^2\gamma + a^2\sin^2\gamma\right)}$$

The N observations are set up as follows:

$$
\left[\begin{array}{ccccc}
y_1^2 & x_1y_1 & x_1 & y_1 & 1 \\
y_2^2 & x_2y_2 & x_2 & y_2 & 1 \\
\vdots & \vdots & \vdots & \vdots & \vdots \\
y_N^2 & x_Ny_N & x_N & y_N & 1
\end{array}\right]
\left[\begin{array}{c}
w_1 \\ w_2 \\ w_3 \\ w_4 \\ w_5
\end{array}\right]
=
\left[\begin{array}{c}
-x_1^2 \\ -x_2^2 \\ \vdots \\ -x_N^2
\end{array}\right]
\tag{8}
$$

The required parameters (γ, a, b, x_c, y_c) can be obtained by solving the set of equations in Equation 7. First introduce the substitutions:

$$
\begin{aligned}
P &= w_1^2 + w_2^2 - 2w_1 + 1 \\
Q_0 &= -w_4^2 - w_1 w_3^2 + 4w_1 w_5 \\
Q_1 &= w_1^2 w_5 - w_1 w_3^2 + 2w_1 w_5 - w_4^2 + w_5 \\
Q_2 &= w_3 w_4 (w_1 - 1) \sin \gamma \\
Q_3 &= -4w_1^2 w_5 + 6w_1 w_3^2 - 16 w_1 w_5 + 6w_4^2 - 4w_5 \\
R &= b^2 \cos^2 \gamma + a^2 \sin^2 \gamma \\
S &= b^2 \sin^2 \gamma + a^2 \cos^2 \gamma \\
T &= \left(b^2 - a^2\right) \cos \gamma \sin \gamma
\end{aligned}
$$

The required parameters (γ, a, b, x_c, y_c) are given by:

$$
\gamma = 2 \tan^{-1} \left(\frac{w_1 - 1 + \sqrt{P} \pm \sqrt{2}\sqrt[4]{P}\sqrt{w_1 - 1 + \sqrt{P}}}{w_2} \right), \tag{9}
$$

$$
a = \frac{\sqrt{Q_0 - 8Q_1 \cos^6 \gamma + 8Q_2 \cos^5 \gamma + 12 Q_1 \cos^4 \gamma - 8Q_2 \cos^3 \gamma + Q_3 \cos^2 \gamma + 2Q_2 \cos \gamma}}{2 \left(w_1 \cos^2 \gamma + \cos^2 \gamma - w_1\right) \sqrt{w_1 \cos^2 \gamma + \cos^2 \gamma - 1}}, \tag{10}
$$

$$
b = \frac{\sqrt{Q_0 - 8Q_1 \cos^6 \gamma + 8Q_2 \cos^5 \gamma + 12 Q_1 \cos^4 \gamma - 8Q_2 \cos^3 \gamma + Q_3 \cos^2 \gamma + 2Q_2 \cos \gamma}}{2 \left(w_1 \cos^2 \gamma + \cos^2 \gamma - 1\right) \sqrt{w_1 \cos^2 \gamma + \cos^2 \gamma - w_1}}, \tag{11}
$$

$$
x_c = \frac{1}{2} \left(\frac{R\left(w_4 T - w_3 S\right)}{RS - T^2} \right), \tag{12}
$$

$$
y_c = \frac{1}{2} \left(\frac{R\left(w_3 T - w_4 R\right)}{RS - T^2} \right) \tag{13}
$$

$$
\tag{14}
$$

3 Transforming elliptical data

Using the estimated ellipse parameters the data can be transformed into a circle by a single rotation (α) about a vector ($\mathbf{k}$) from the center of the ellipse along its minor axis (b) which also forms the radius of the circle. From the ellipse fitting procedure we know the angle γ that the vector $\mathbf{k}$ makes with the y-axis, see Figure 20

$$
\mathbf{k} = -\sin \gamma \hat{\mathbf{x}} + \cos \gamma \hat{\mathbf{y}}
$$

The desired angle α is given by:

$$
\alpha = \cos^{-1} \left(\frac{a}{b} \right) \tag{15}
$$

Using the general result from "Robot Manipulators: Mathematics, Programming, and Control" by R. P. Paul, MIT Press, 1981 we have that the transformation matrix associated with this

rotation is given by:

$$K = \begin{bmatrix} 1 - \cos^2\gamma + \cos\alpha\cos^2\gamma & \sin\gamma\cos\gamma\cos\alpha - \sin\gamma\cos\gamma & \cos\gamma\sin\alpha & 0 \\ \sin\gamma\cos\gamma\cos\alpha - \sin\gamma\cos\gamma & \cos^2\gamma - \cos\alpha\cos^2\gamma + \cos\alpha & \sin\gamma\sin\alpha & 0 \\ -\cos\gamma\sin\alpha & -\sin\gamma\sin\alpha & \cos\alpha & 0 \\ 0 & 0 & 0 & 1 \end{bmatrix}$$

(16)

4   Determining yaw and pitch angles

The yaw (ψ) and pitch (ϕ) angles of the vehicle can be determined from the fitted ellipse. The transformation of the measured data point (x_i', y_i', z_i') to the point on the circle (x_i, y_i, z_i) can either be performed by:

1. rotation of α about vector k, as above, or

2. rotation of ϕ about the x-axis and then ψ about the y-axis.

where as previously

$$\alpha = \cos^{-1}\frac{a}{b}$$

For a rotation of ϕ about the x-axis we have:

$$\text{Pitch} = \begin{bmatrix} 1 & 0 & 0 & 0 \\ 0 & \cos\phi & -\sin\phi & 0 \\ 0 & \sin\phi & \cos\phi & 0 \\ 0 & 0 & 0 & 1 \end{bmatrix}$$

(17)

For a rotation of ψ about the new y-axis

$$\text{Yaw} = \begin{bmatrix} \cos\psi & 0 & \sin\psi & 0 \\ 0 & 1 & 0 & 0 \\ -\sin\psi & 0 & \cos\psi & 0 \\ 0 & 0 & 0 & 1 \end{bmatrix}$$

(18)

Therefore the combined transformation matrix is:

$$YP = [\text{Yaw}][\text{Pitch}] = \begin{bmatrix} \cos\psi & \sin\psi\sin\phi & \sin\psi\cos\phi & 0 \\ 0 & \cos\phi & -\sin\phi & 0 \\ -\sin\psi & \cos\psi\sin\phi & \cos\psi\cos\phi & 0 \\ 0 & 0 & 0 & 1 \end{bmatrix}$$

(19)

Thus the required angles can be obtained from equating the matrices in 16 and 19. Using the trace of both matrices gives one equation as follows:

$$\cos\psi + \cos\phi + \cos\psi\cos\phi + 1 = 2 + 2\cos\alpha$$

(20)

and equating the differences between the elements on the respective off-diagonals of the two matrices ($YP[3,1] - YP[1,3] = K[3,1] - K[1,3]$) and ($YP[3,2] - YP[2,3] = K[3,2] - K[2,3]$) gives the following:

$$-\sin\psi - \sin\psi\cos\phi = -2\sin\gamma\sin\alpha$$

(21)

$$\sin\phi + \cos\psi\sin\phi = -2\sin\gamma\sin\alpha$$

(22)

Solving for ϕ and ψ using Equations 20 and 21 yields:

$$\psi = 2\tan^{-1}\left(\frac{\cos\gamma\sin\alpha}{1+\cos\alpha}\right) \tag{23}$$

$$\phi = \cos^{-1}\left(\frac{1-\cos\psi+2\cos\alpha}{1+\cos\psi}\right) \tag{24}$$

while using Equations 20 and 22 yields:

$$\psi = \cos^{-1}\left(\frac{2\sin\gamma\sin\alpha-\cos\psi}{\sin\psi}\right) \tag{25}$$

$$\phi = -2\tan^{-1}\left(\frac{\sin\gamma\sin\alpha}{1+\cos\alpha}\right) \tag{26}$$

5   Applying center correction to data in cylindrical coordinates

Figure 21 shows the geometry of the correction required to be applied to a measurement (x_i, y_i) taken from a position not in the center of the pipe.

The center of the pipe is given by the coordinates (x_c, y_c) from the current position. The known parameters are the angle θ_i and the measured radius (r_i). It is desired to convert these parameters into those at the center of the pipe ($\hat{r}_i$, $\hat{\theta}_i$). The corrections required are:

$$\hat{r}_i = \sqrt{r_i^2 + r_c^2 + 2r_c r_i \cos(\lambda - \theta_i)} \tag{27}$$

$$\hat{\theta}_i = \theta_i - \cos^{-1}\left(\frac{r_i^2 + \hat{r}_i^2 - r_c^2}{2r_i\hat{r}_i}\right) \tag{28}$$

$$\hat{\theta}_i = \sin^{-1}\left(\frac{r_c\sin(\lambda-\theta_i)}{\hat{r}_i}\right) - \theta_i \tag{29}$$

$$\tag{30}$$

where λ is the angle between the nominal horizontal given by $\lambda = \tan^{-1}\left(\frac{y_c}{x_c}\right)$, and r_c is the distance from the current position (x_c, y_c) to the center of the pipe given by $r_c = \sqrt{x_c^2 + y_c^2}$.

– 50 –

CLAIMS:

1.   An inspection system for a conduit comprising measurement means for travelling in said conduit and obtaining data on said conduit, and processing means for processing
5   said data to identify regions of said conduit corresponding to defects in said conduit.

2.   An inspection system as claimed in claim 1, wherein said processing means includes means for extracting dimension data on said conduit from said data obtained by said measurement means.
10

3.   An inspection system as claimed in claim 2, wherein said dimension data comprises a plurality of circumferential data of the inner surface of said conduit, said circumferential data each corresponding to points along the path of travel of said measurement means.
15

4.   An inspection system as claimed in claim 3, wherein said processing means includes movement correction means for adjusting said circumferential data to account for movement of said measurement means within said conduit.

20 5.   An inspection system as claimed in claim 2, wherein said processing means includes segmentation means for processing said dimension data into segments which represent regions which could correspond to defects in said conduit.

6.   An inspection system as claimed in claim 5, wherein said processing means
25   includes image preprocessing means for generating a grid map of depth values corresponding to the inner surface of said conduit from said dimension data, said grid map providing an image of said surface with pixels of said image having a corresponding depth value.

30 7.   An inspection system as claimed in claim 6, wherein said segmentation means includes feature extraction means for generating feature data and forming a feature vector with the feature data for each pixel.

8.   An inspection system as claimed in claim 7, wherein said segmentation means includes means for determining pixels of interest from the feature vectors and assigning respective labels to predetermined types of said pixels of interest.

5   9.   An inspection system as claimed in claim 8, wherein said segmentation means includes means for forming said segments by grouping said pixels of interest having said labels which are similar into said regions.

10.   An inspection system as claimed in claim 5, wherein said processing means 10   includes classification means for processing said segments so as to classify said segments as corresponding to predetermined features of said conduit.

11.   An inspection system as claimed in claim 10, wherein said classification means includes a neural network classifier for classifying said segments.

15

12.   An inspection system as claimed in claim 11, wherein said classification means includes means for filtering said segments, means for rescaling the filtered segments, means for transforming the rescaled segments from a spatial domain to a power domain, and means for wedge–ring sampling the transformed segments for application t the 20   neural network classifier.

13.   An inspection system as claimed in claim 11, wherein said neural network classifier includes a plurality of neural networks for determining whether said segments correspond to one of a plurality of predetermined features, respectively.

25

14.   An inspection system as claimed in claim 10, wherein said processing means includes interpretation means for processing a classified segment to obtain attributes of the corresponding feature for identifying said feature on the basis of said attributes and feature data.

30

15.   An inspection system as claimed in claim 1, wherein said measurement means includes laser scanning means.
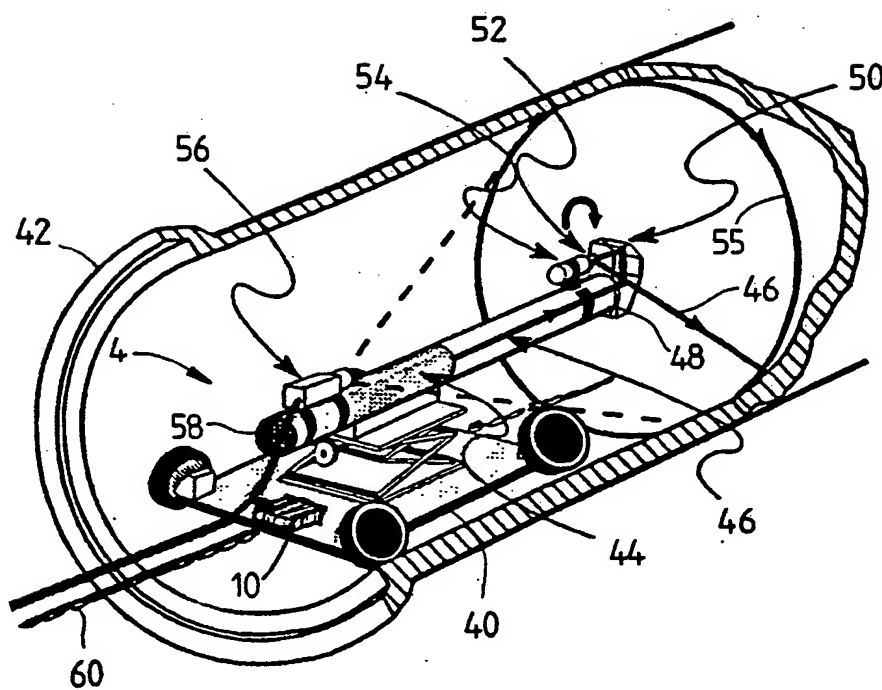
- 52 -

16. .   An inspection system as claimed in claim 1 or 15, wherein said measurement means includes sonar scanning means.

17.   An inspection system as claimed in claim 1 or 4, wherein said measurement
5   means includes means for detecting the position and orientation of said measurement means in said conduit.

18. .   An inspection system as claimed in claim 15, wherein said laser scanning means includes a laser, means for circulating a beam generated by the laser against the surface
10   of said conduit, and camera means for producing image data representative of areas illuminated by said beam.

19.   An inspection system as claimed in claim 17, wherein said processing means includes means for extracting, from said image data, position data for pixels of a laser
15   trace produced by said beam.

20.   An inspection system as claimed in claim 16, wherein said sonar scanning means includes a rotating sonar transducer for emitting sonar signals to and receiving sonar echoes from the inner surface of said conduit.

20

21.   An inspection system as claimed in claim 20, wherein said processing means includes means for obtaining r,θ dimension data on said inner surface from said sonar echoes by performing curve analysis on said sonar echoes and monitoring the angular position of said rotating sonar transducer.

25
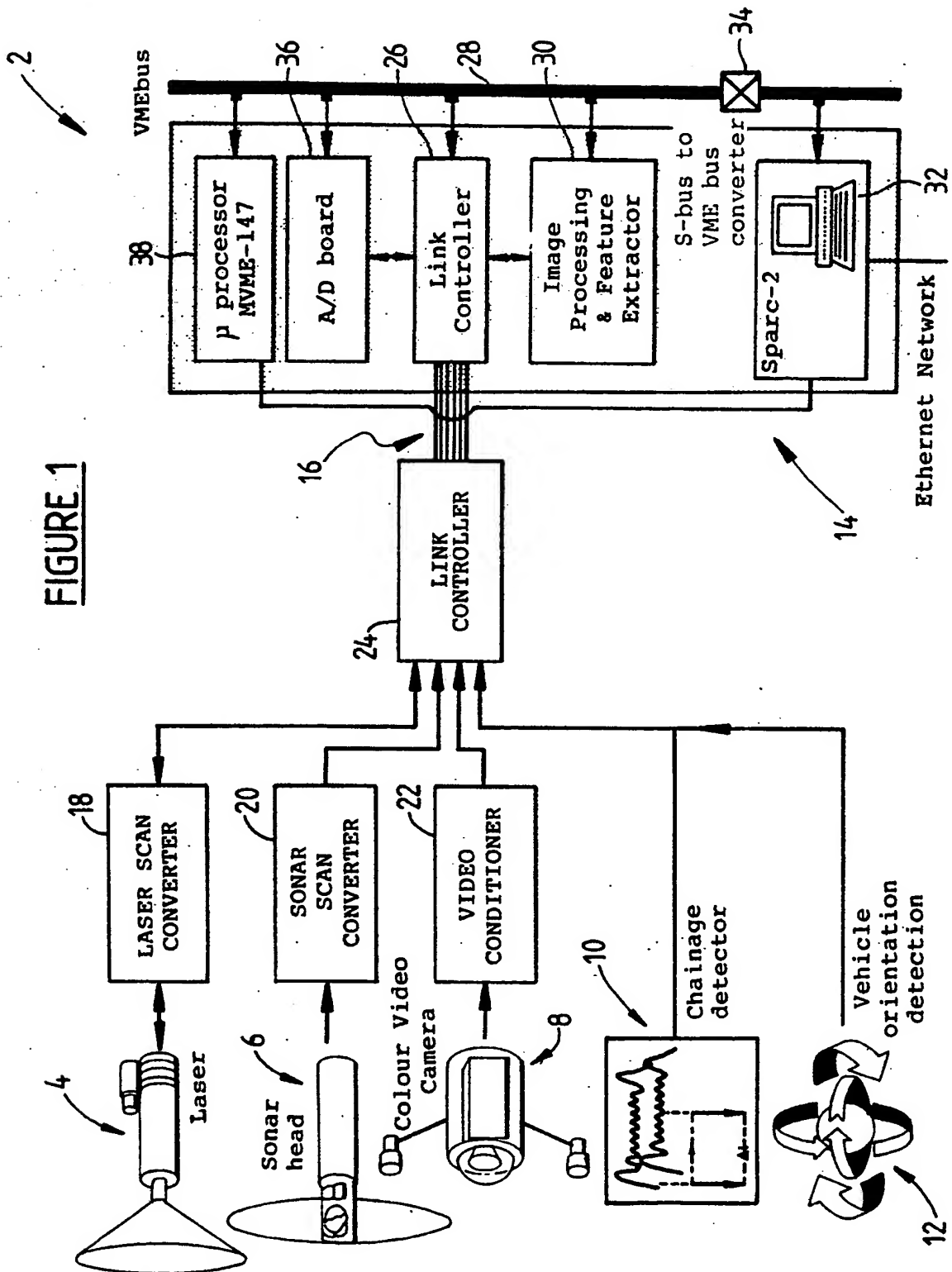
FIGURE 1

FIGURE 2

3/19

FIGURE 3

4/19
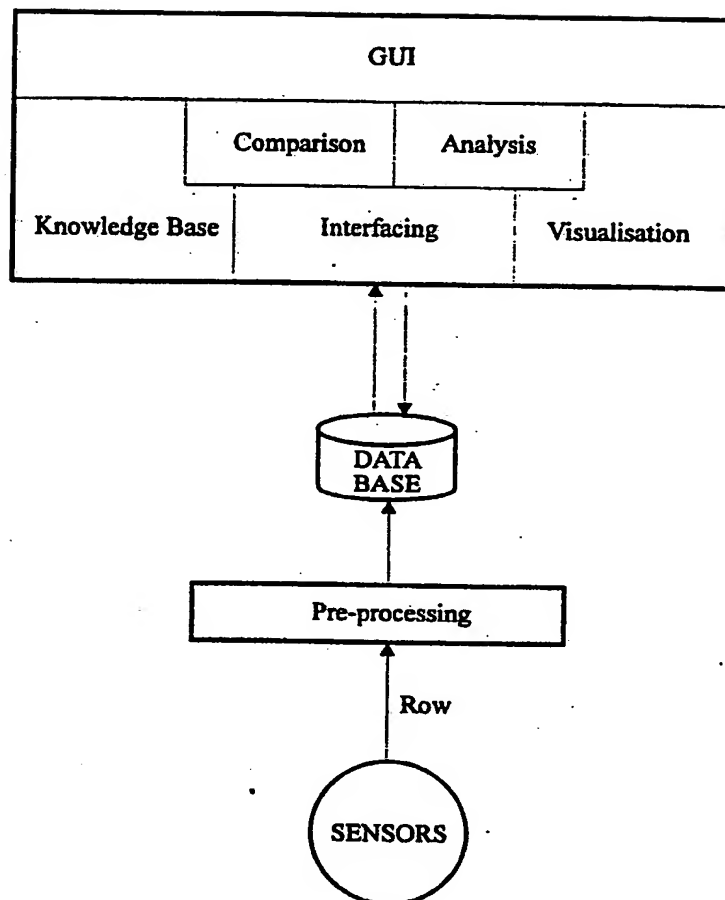
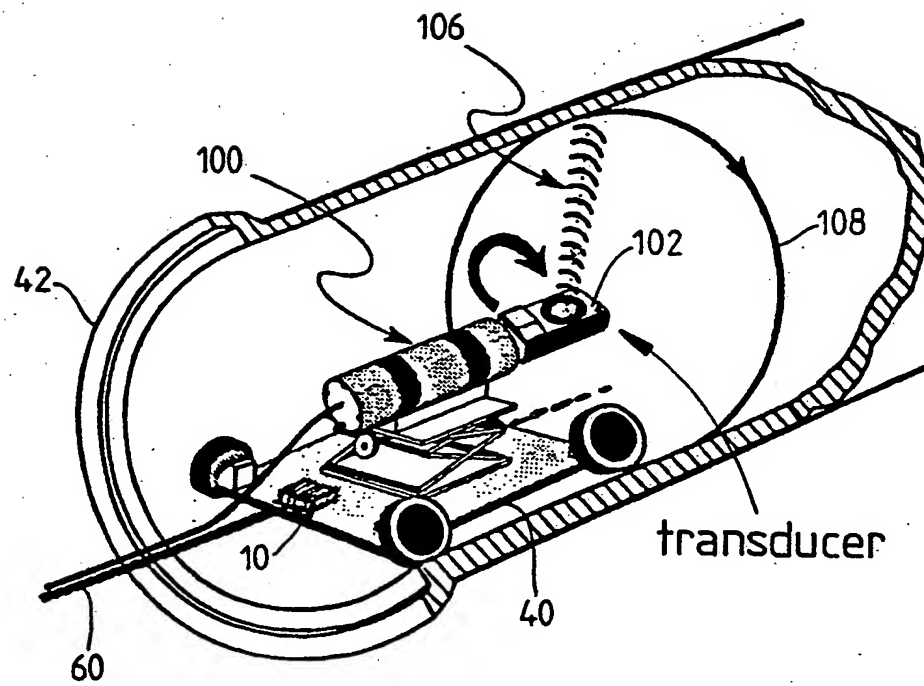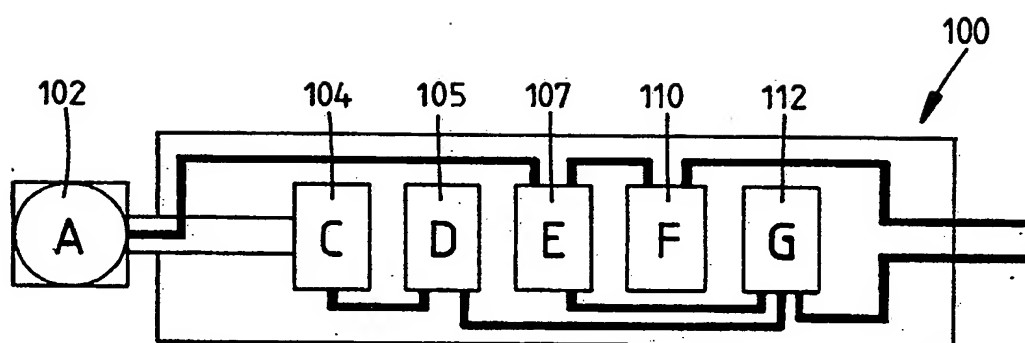FIGURE 4
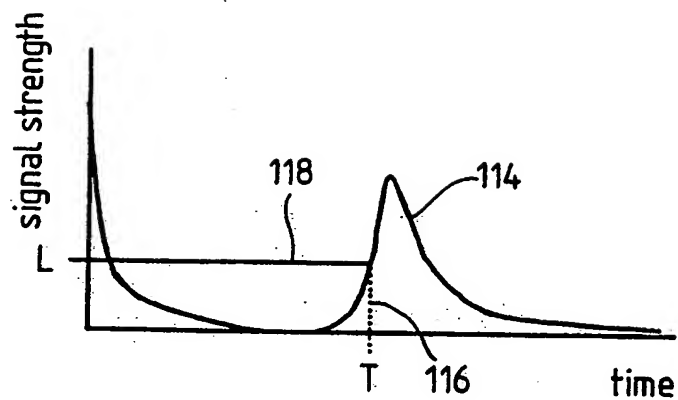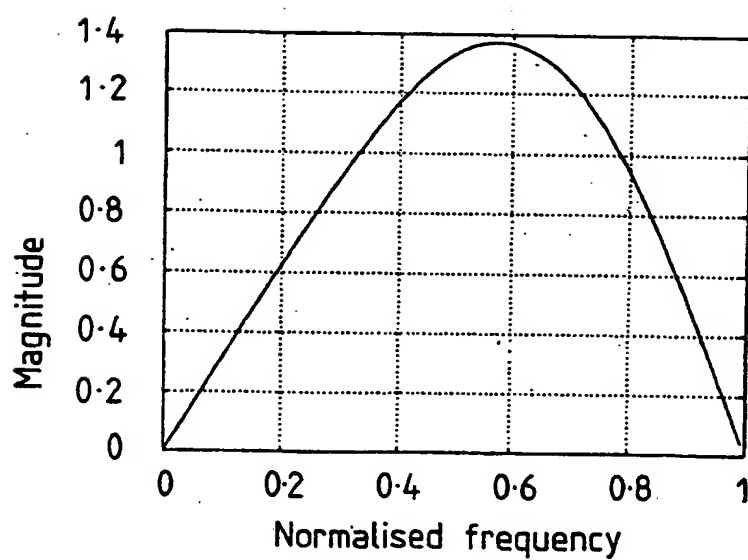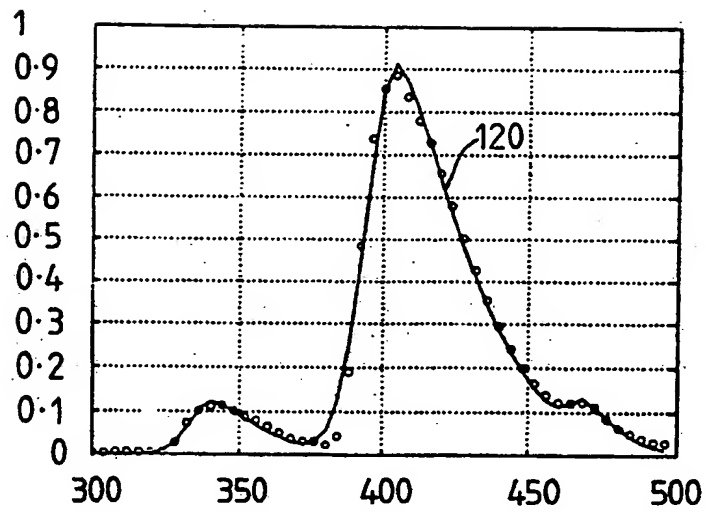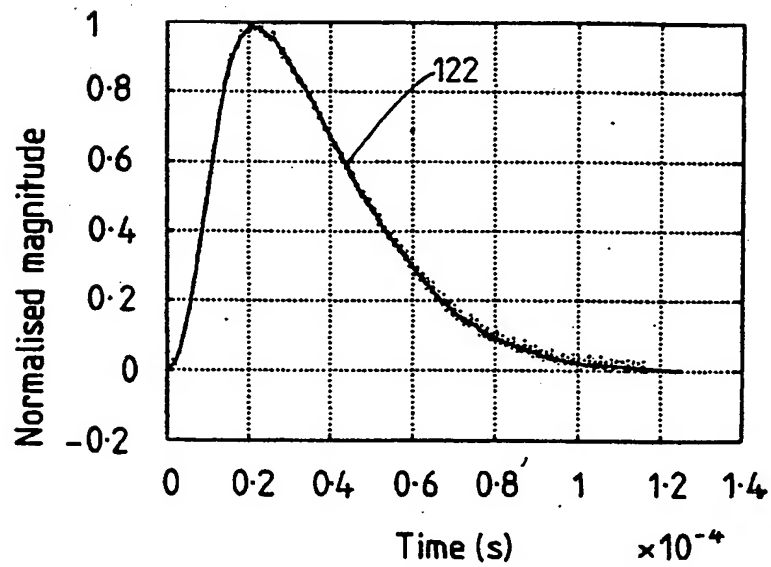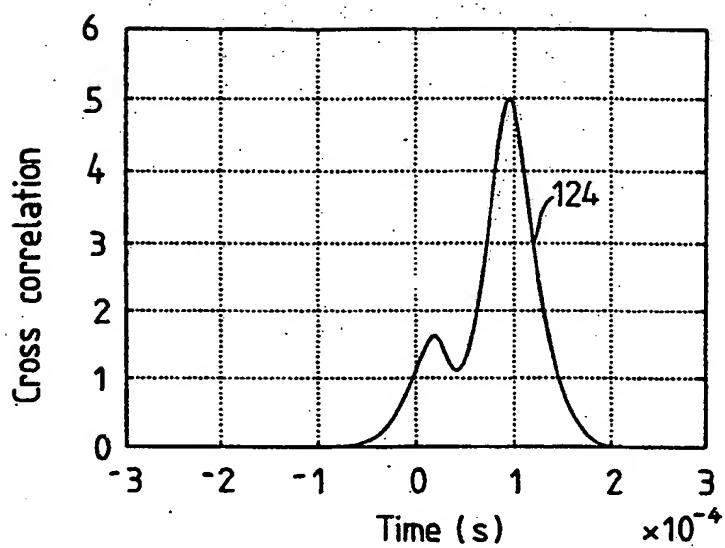
FIGURE 5

FIGURE 6

FIGURE 7

FIGURE 8

FIGURE 9

FIGURE 10

FIGURE 11

FIGURE 12

200

```
┌─────────────────────────────┐
│    feature extraction       │──── 220
└─────────────────────────────┘
              │
              ▼
┌─────────────────────────────┐
│      pixel labelling        │──── 222
└─────────────────────────────┘
              │
              ▼
┌─────────────────────────────┐
│     region extraction       │──── 224
└─────────────────────────────┘
```

FIGURE 13

204

```
┌─────────────────────────────────┐
│      defect map filter          │──── 230
└─────────────────────────────────┘
                │
                ▼
┌─────────────────────────────────┐
│        interpolation            │──── 232
└─────────────────────────────────┘
                │
                ▼
┌─────────────────────────────────┐
│      Fourier transform          │──── 234
└─────────────────────────────────┘
                │
                ▼
┌─────────────────────────────────┐
│      wedge-ring sampling        │──── 236
└─────────────────────────────────┘
                │
                ▼
┌─────────────────────────────────┐
│       neural network            │──── 238
│       classification            │
└─────────────────────────────────┘
```
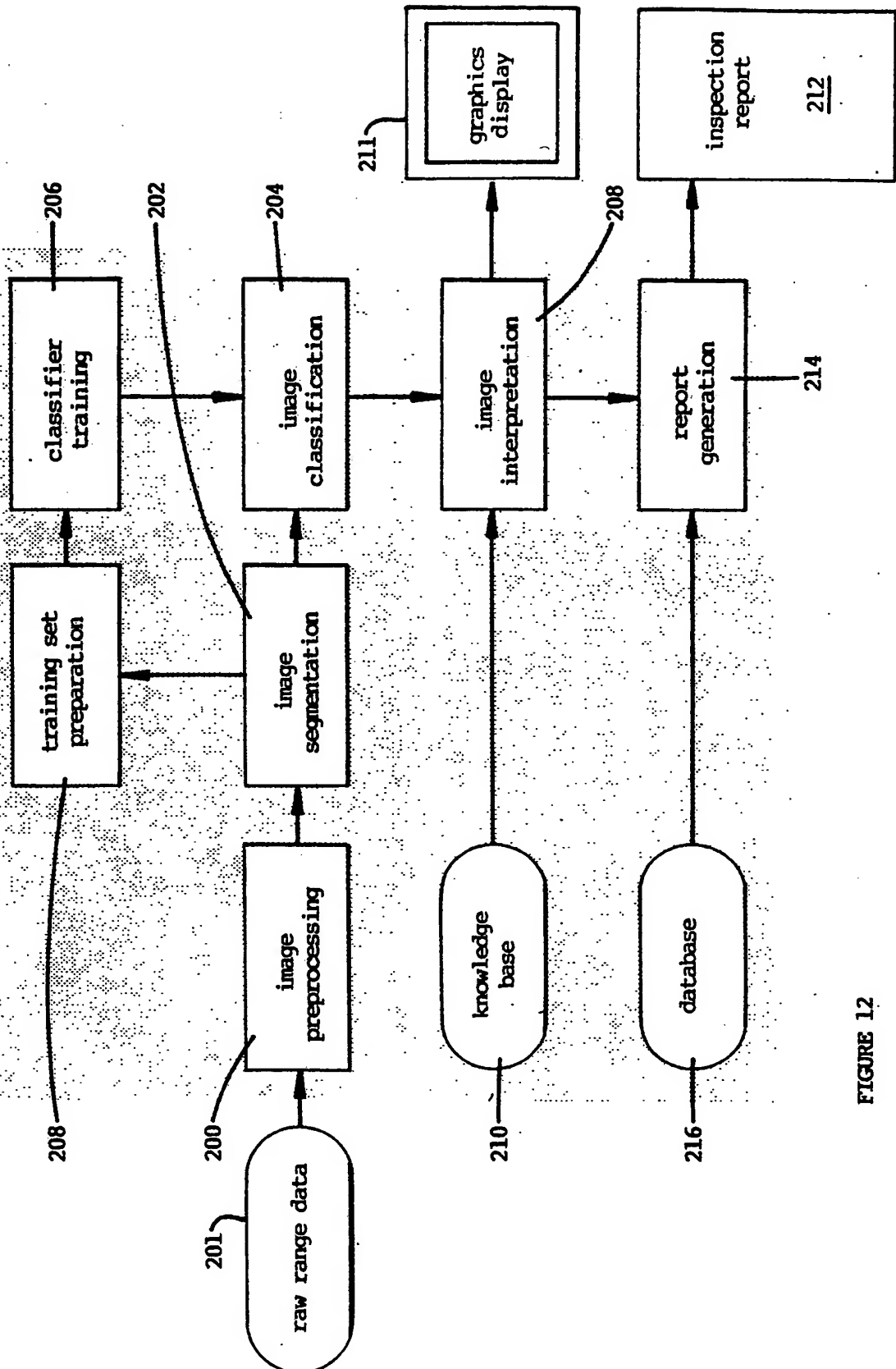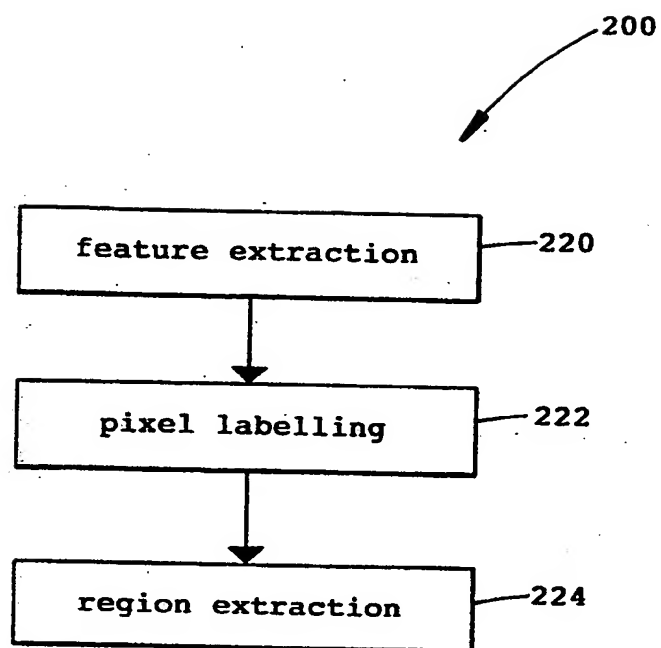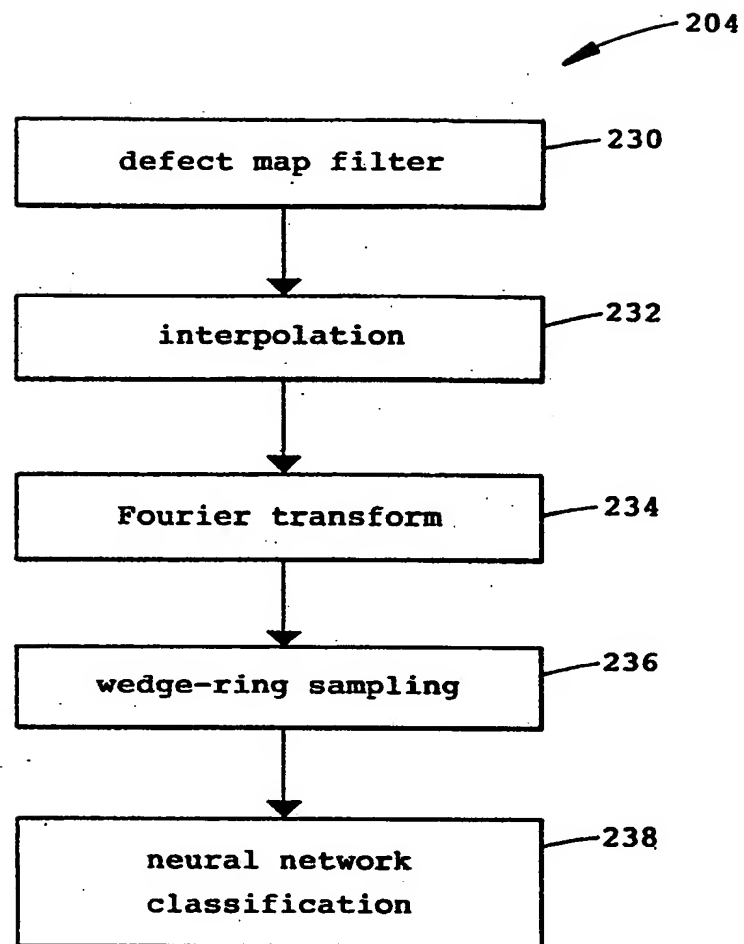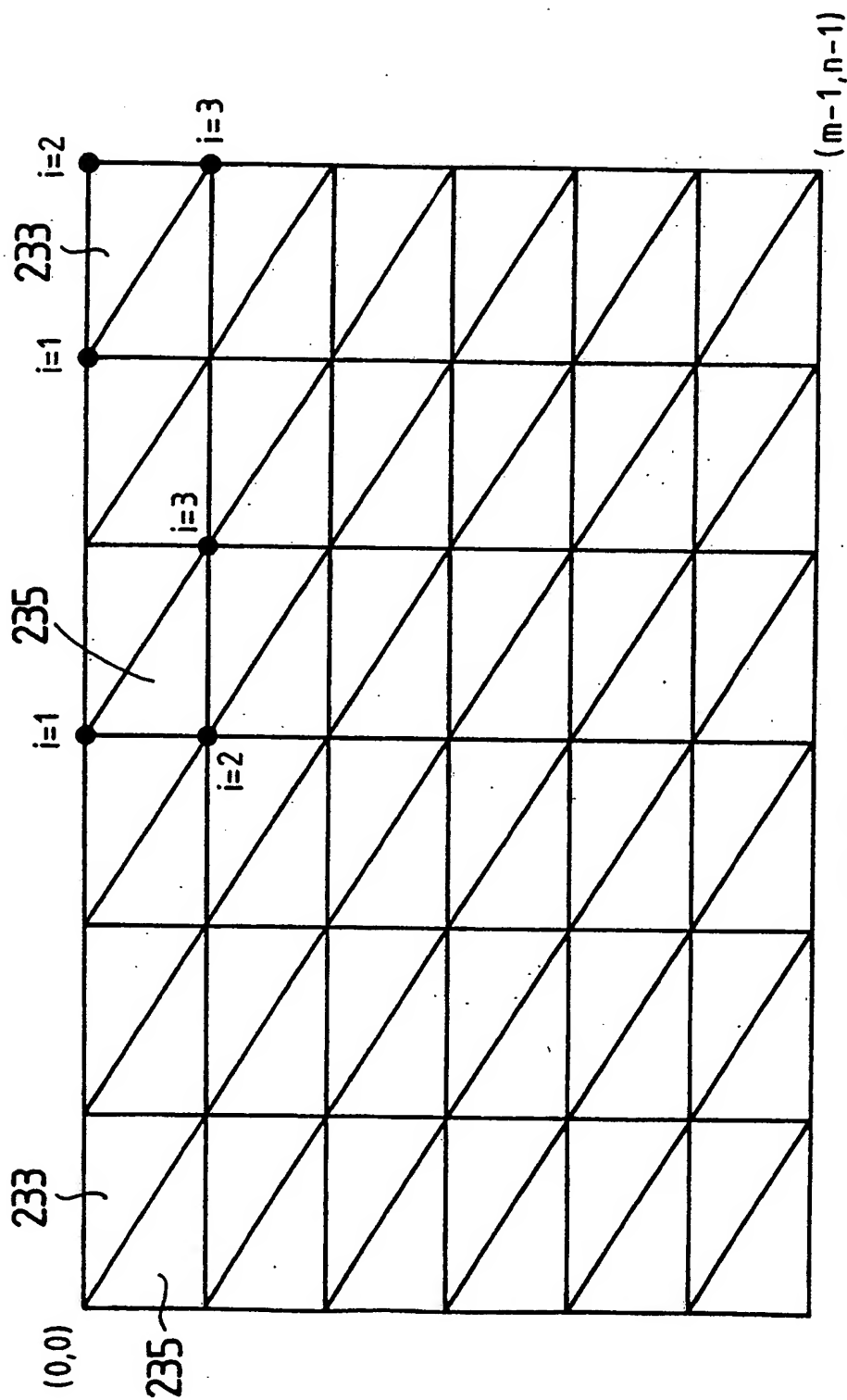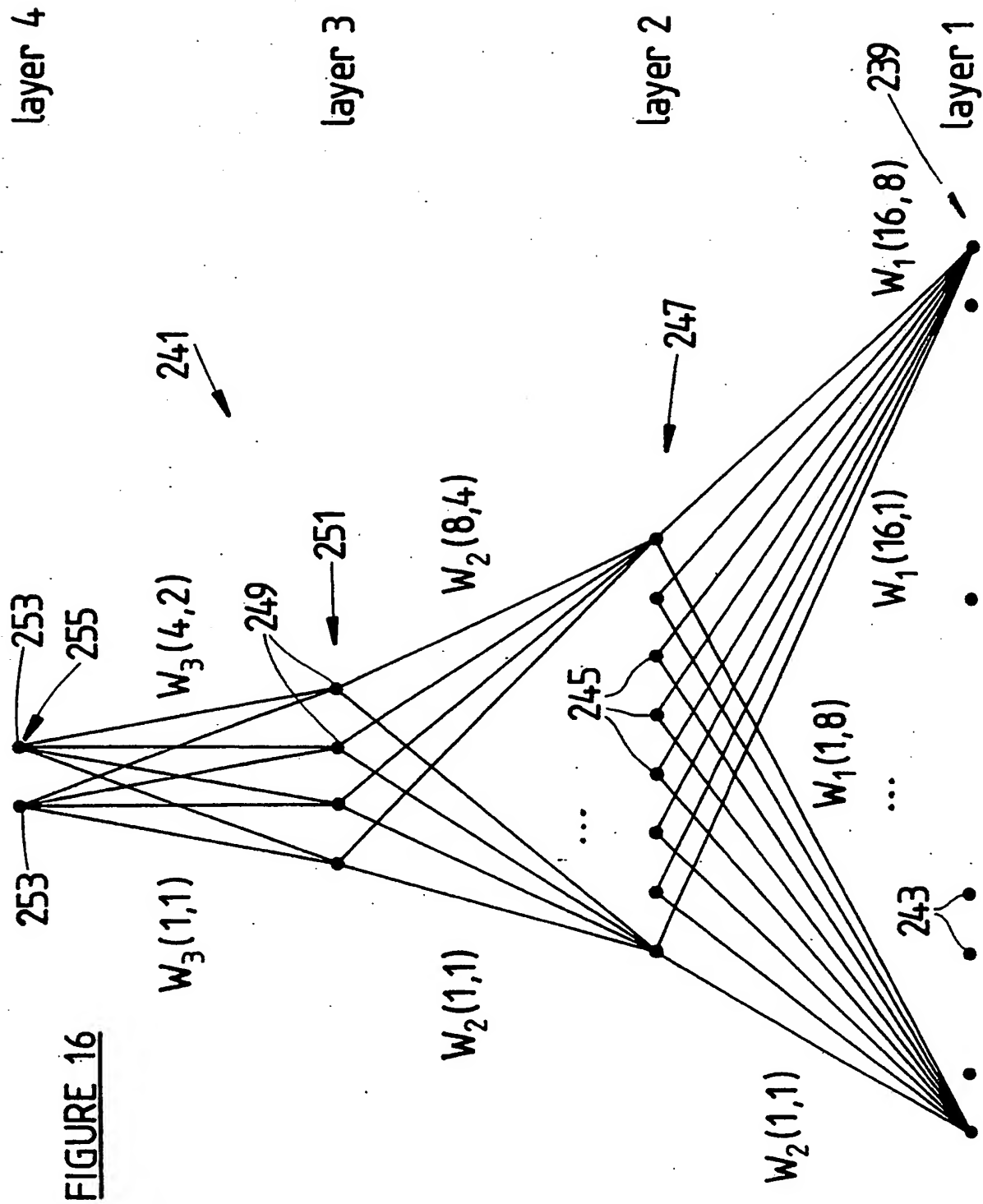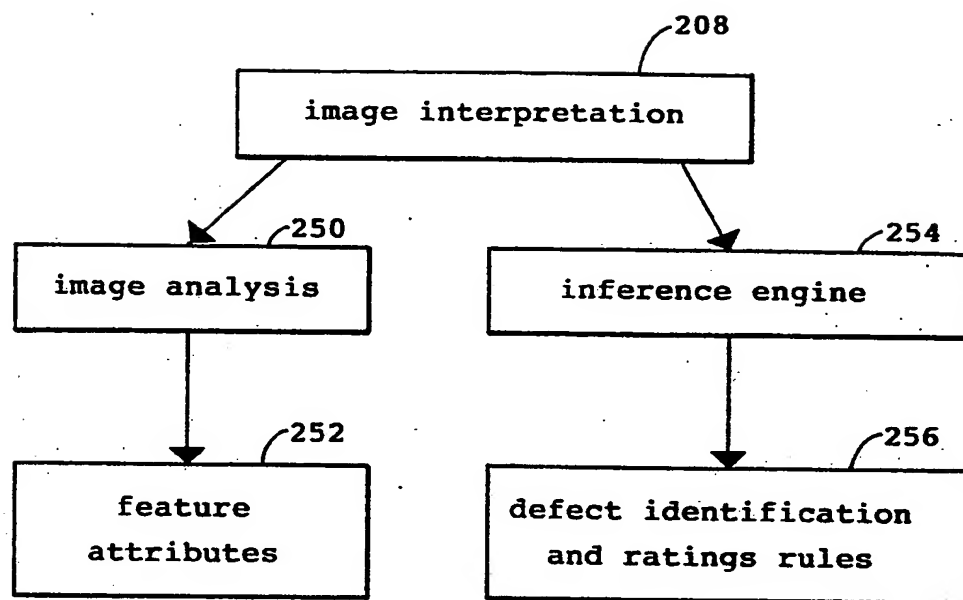
FIGURE 14
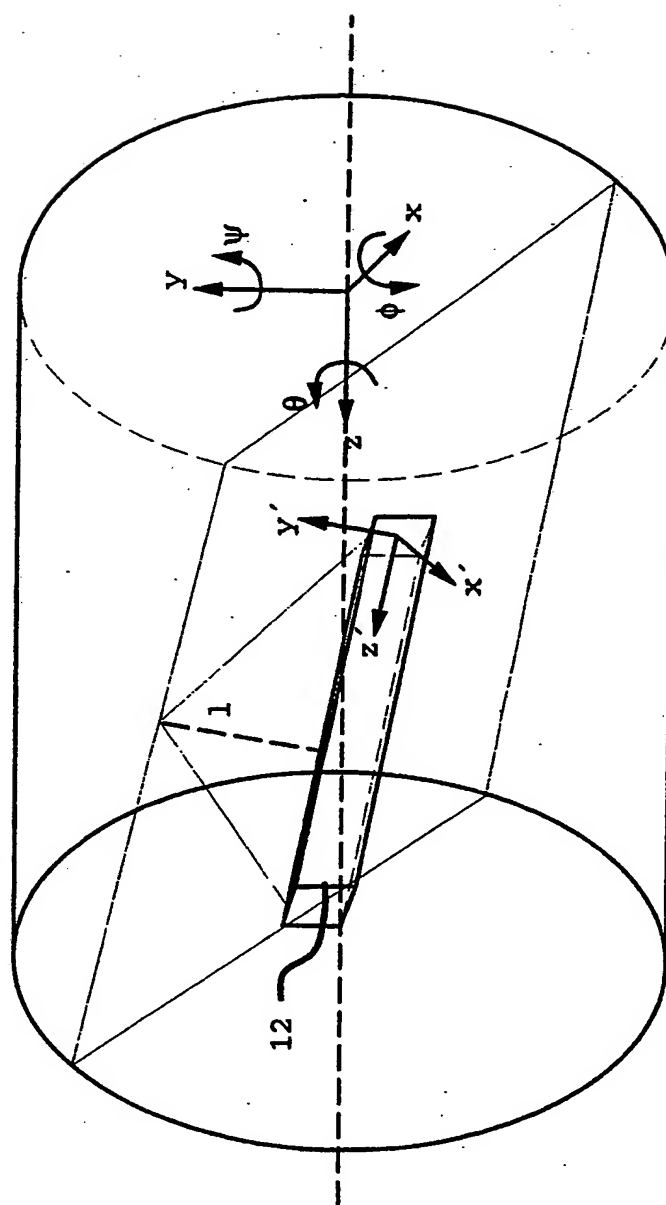
FIGURE 15

FIGURE 16
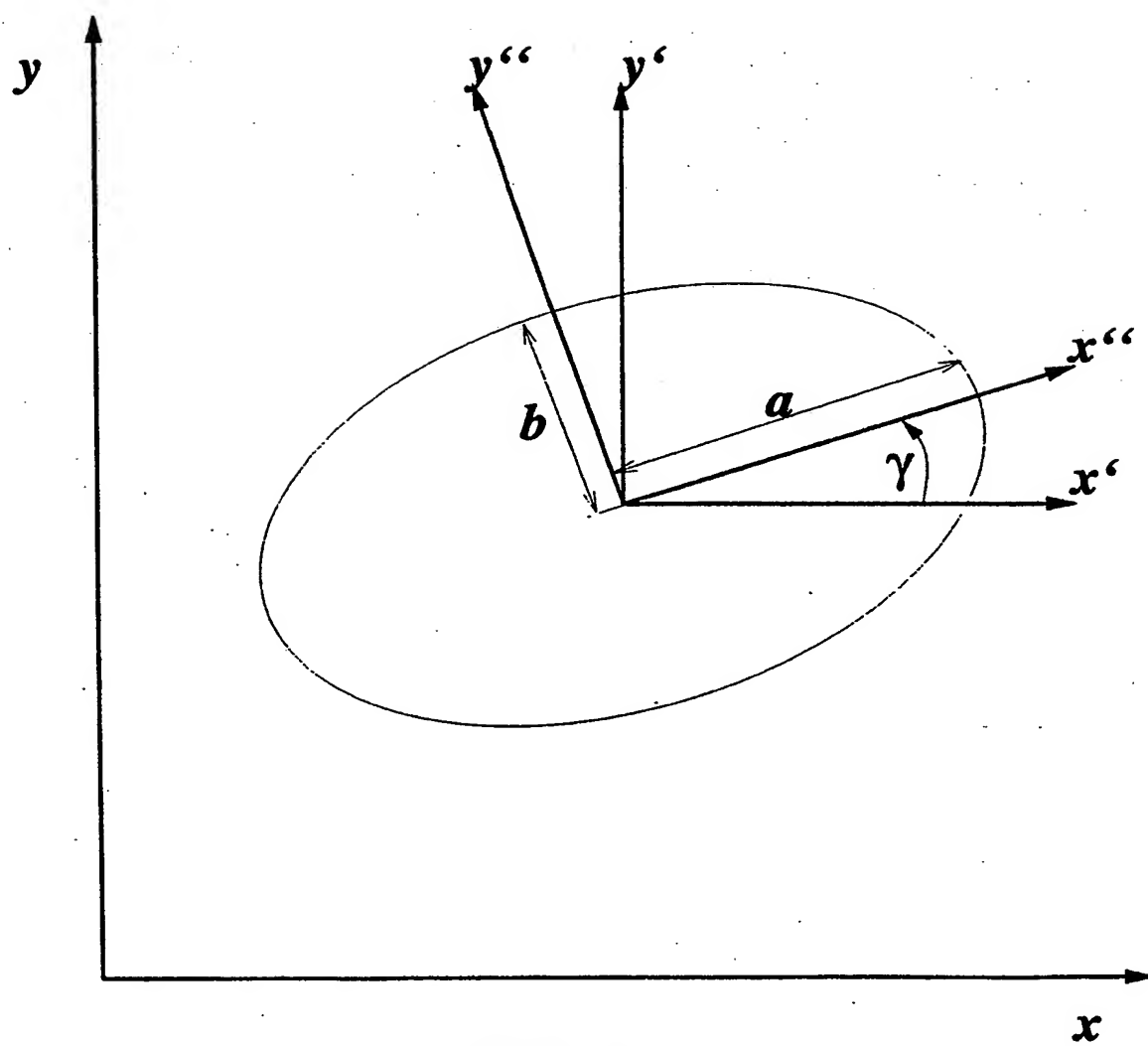
FIGURE 17

FIGURE 18

FIGURE 19

FIGURE 20

19/19
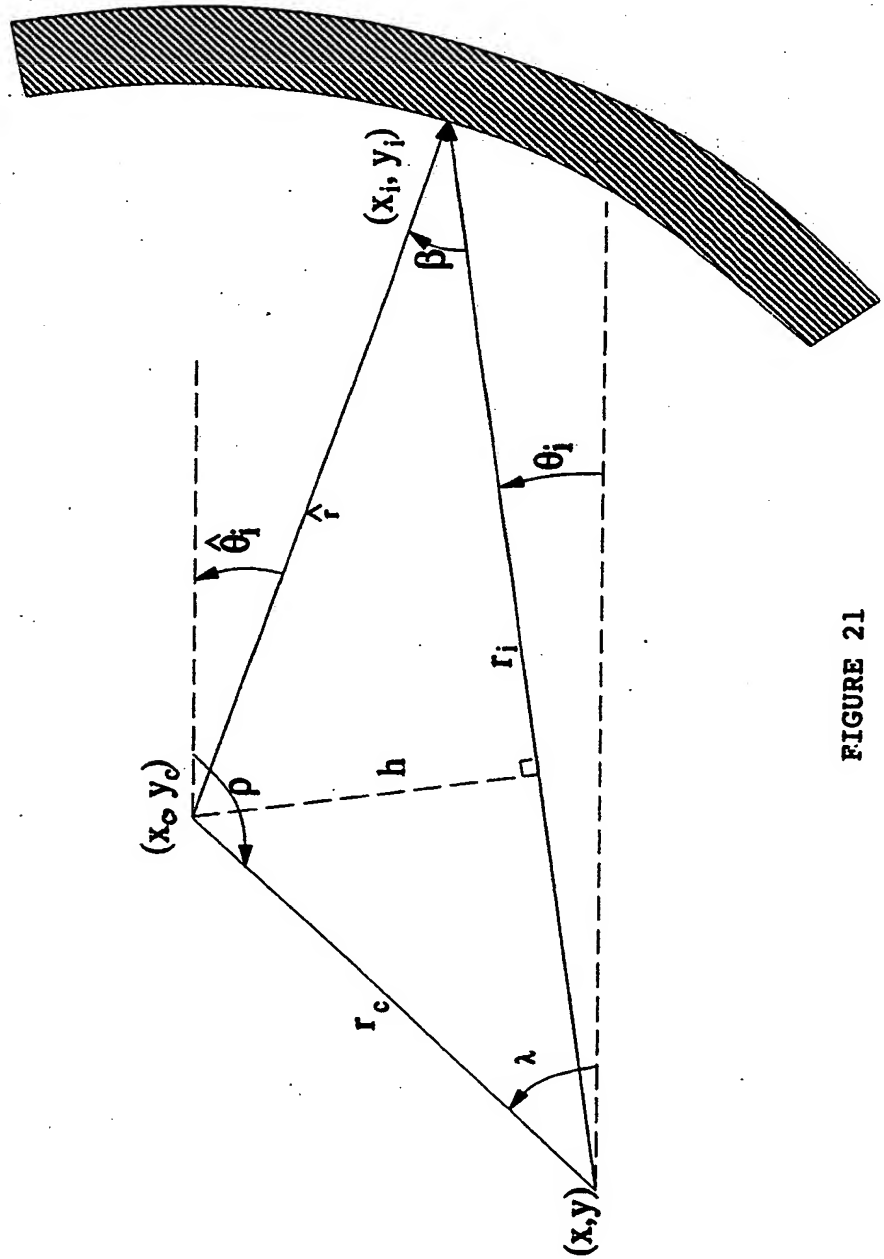
FIGURE 21

A. **CLASSIFICATION OF SUBJECT MATTER**	
Int. Cl.[6] G01C 7/06, G01N 21/88, 29/10, G01M 3/00, 3/38	

According to Internati nal Patent Classification (IPC) or to both national classification and IPC

B. **FIELDS SEARCHED**

Minimum documentation searched (classification system followed by classification symbols)
IPC : G01C 7/06, 7/00, G01M 3/00, 3/38, G01N 21/88, 29/04, 29/10

Documentation searched other than minimum documentation to the extent that such documents are included in the fields searched
AU : IPC as above and F17D 5/02, 5/06

Electronic data base consulted during the international search (name of data base, and where practicable, search terms used)
DERWENT : G01N 21/88, 29/10, 29/04, G01M 3/00 & keywords
& JAPIO : (CONDUIT# or PIP: or TUB:) and (RADIUS: or DIAMET: or DIMENSION: or DISTANCE#)

C.	**DOCUMENTS CONSIDERED TO BE RELEVANT**	
Category*	Citation of document, with indication, where appropriate, of the relevant passages	Relevant to Claim No.
Y,X	GB,A, 2102565 (DRAFTRULE LIMITED) 2 February 1983 (02.02.83) Abstract, page 1	1-5,15-21
Y,X	GB,A, 2094470 (J.W. van DYK) 15 September 1982 (15.09.82) Abstract	1-5,15-21
X	WO,A1, 86/03295 (WETTERVIK et al) 5 June 1986 (05.06.86) Abstract	1,17
X	EP,A2, 504591 (DENSO-CHEMIE WEDEKIND KG) 23 September 1992 (23.09.92) Abstract	1,17

[X] Further documents are listed
in the continuation of Box C.

[X] See patent family annex.

*	Special categories of cited documents :	"T"	later document published after the international filing date or priority date and not in conflict with the application but cited to understand the principle or theory underlying the invention
"A"	document defining the general state of the art which is not considered to be of particular relevance		
"E"	earlier document but published on or after the international filing date	"X"	document of particular relevance; the claimed invention cannot be considered novel or cann t be considered to involve an inventive step when the document is taken alone
"L"	document which may throw doubts on priority claim(s) or which is cited to establish the publication date of another citation or other special reason (as specified)	"Y"	document of particular relevance; the claimed invention cannot be considered to involve an inventive step when the document is combined with one or more other such documents, such combination being obvious to a person skilled in the art
"O"	document referring to an oral disclosure, use, exhibition or other means		
"P"	document published prior to the international filing date but later than the priority date claimed		
		"&"	document member of the same patent family

Date of the actual completion of the international search	Date of mailing of the international search report
27 October 1994 (27.10.94)	4 Nov 1994 (4.11.94)
Name and mailing address of the ISA/AU AUSTRALIAN INDUSTRIAL PROPERTY ORGANISATION PO BOX 200 WODEN ACT 2606 AUSTRALIA	Authorized fficer M. DIXON
Facsimile No. 06 2853929	Telephone No. (06) 2832194

C(Continuation).	DOCUMENTS CONSIDERED TO BE RELEVANT	
Category*	Citation of document, with indication, where appr priate of the relevant passages	Relevant to Claim N .
X,Y	EP,A2, 282687 (NIPPON KOKAN KABUSHIKI KAISHA) 21 September 1988 (21.09.88) Col 1 - Col 3 line 13	1-5,15-21
X	EP,A1, 51912 (BRITISH GAS CORPORATION) 19 May 1982 (19.05.82) Abstract	1-5,17
A	US,A, 4868648 (NOBUNAGA) 19 September 1989 (19.09.89) Abstract	

This Annex lists the known "A" publication level patent family members relating to the patent documents cited in the above-mentioned international search report. The Australian Patent Office is in no way liable for these particulars which are merely given for the purpose of information.

Patent Document Cited in Search Report		Patent Family Member						
WO	8603295	AT	67850	CA	1272778	DE	3584254	
		DK	3424/86	EP	229762	FI	871640	
		JP	62501796	NO	863019	SE	8406065	
		US	4913558					
EP	504591	DE	9103527					
EP	282687	DE	3884242	JP	63231260			
EP	51912	AU	75981/81	CA	1166002	DE	3174184	
		EP	51912	GB	2088059	JP	57088310	
		NO	812763	US	4443948	ZA	8105628	

END OF ANNEX